A Major Qualifying Project

Submitted to the Faculty of

WORCESTER POLYTECHNIC INSTITUTE

in fulfillment of the requirements for the

degree of Bachelor of Science

By:

Jackson Brandin, Jacob Spada, Matthew Woods

Project Advisor:

Prof. Sneha P. Narra

Worcester Polytechnic Institute

Worcester, Massachusetts

Date:

May 16, 2020

Abstract

This project focuses on a subset of additive manufacturing processes known as the laser powder bed fusion (LPBF) process. To expand the materials that can be used within these machines, experimental trials must be done, however, working with a commercial LPBF printer outside of its material capabilities, parameter windows, and retrofitting with monitoring equipment can void the warranty on a machine that could bear heavy on costs, on the order of hundreds of thousands of dollars. To address these limitations, we are tasked with designing and fabricating an economical LPBF prototype chamber for experimentation with various metal alloy powders and chamber gases while accommodating the addition of monitoring equipment.

Table of Contents

List of Figures

List of Tables

Table of Nomenclature

Abbreviation	Definition
LPBF	Laser Powder Bed Fusion
AM	Additive Manufacturing
CAD	Computer Aided Design
EBM	Electron Beam Melting
Galvo	Galvanometer
PBF	Powder Bed Fusion
SLA	Stereolithography Apparatus
SLM	Selective Laser Melting
SLS	Selective Laser Sintering

1.0 Introduction

Since the invention of the first three-dimensional printer in 1983, the technology of 3D printing has been rapidly expanding. As the need for lean manufacturing grows, additive manufacturing (AM) will play a key role in reducing waste. AM is an innovative type of manufacturing that uses different processes to deposit materials in layers to form a 3-dimensional object. This means that additive manufacturing has less waste compared to traditional manufacturing methods such as machining. Other benefits of additive manufacturing include rapid prototype production at very minimal material costs for certain polymer-based processes. There are seven main types of additive manufacturing categories which include material extrusion, material jetting, VAT photopolymerization, direct energy deposition, binder jetting, sheet lamination, and powder bed fusion (Nichols, 2017).

This project focuses on a subset of additive manufacturing called powder bed fusion (PBF) processes which involve a fine powder substance that is laid over a build area (layer thickness on the order of tens of microns), and then solidified in layers using a high power-density laser or electron beam based on input from a CAD model (Goodridge and Ziegelmeier, 2017). This PBF process can be further divided into laser powder bed fusion (LPBF) and electron beam powder bed fusion, popularly known as electron beam melting (EBM) (Bartolo et al., 2017). LPBF uses a high power-density laser beam to selectively melt the powder layers that are 20 to 60 microns thick (Leary, 2017). This enable the fabrication of fine features and complex geometries. While the advent of AM processes has made great strides in becoming economical and efficient, there are still challenges that must be addressed to make it a suitable large-scale manufacturing method.

LPBF systems range greatly in capital costs depending on size and technology capabilities but most industrial grade systems are within the scope of ~$1 M (DigitalAlloy, 2019). This means operating these machines out of the confines of a warranty could cost the operator upwards of $1M. This would include using gases and metal powders that are not known to be compatible with the LPBF machine, retrofitting the equipment with sensors and imaging capabilities, and changing processing conditions. However, to further the capabilities of LPBF processes and understand how certain metal alloys interact with the laser, experimental trials must occur.

2.0 Background

2.1 Additive Manufacturing

Compared to conventional subtractive manufacturing practices, which relies on starting with a bulk material and reducing that material into the desired shape, AM majorly only uses the required material. AM also delivers a shorter production time. This leads to a further increase in reducing costs in manufacturing. In modern era, the need for reducing costs and waste is ever more crucial. In 1984 Chuck Hull filed a patent for a Stereolithography Apparatus “SLA”. This patent was specifically for the material used in the plastic 3D printing process, which is an acrylic based photopolymer. Following this, Mr. Hull then created the world's first 3D printing company called 3D systems. 3D systems went on to create the first SLA machine which fabricated complex parts layer by layer. The manufacturing process was relatively short, but the size of the objects was limited. Mr. Hull helped to lay the foundation for further advancements in the additive

manufacturing field. The next breakthrough came from Dr. Carl Deckard, who patented the selective laser sintering (SLS) technology. This process fused powder particles together by use of a laser. This advancement in the SLS process allowed prints to be manufactured out of metal. Over the next decade, AM research expands with further advancements in technology.

Today, there are seven different types of 3D printers. The first process is referred to as Material Jetting. Material jetting operates like 2D printers where printheads dispense droplets of a photosensitive material onto a printing bed that is under an ultraviolet light. The resin needs to be heated to 30 –60 degrees Celsius (B News, 2019). The printer then builds up the part layer-by-layer. Material jetting most commonly uses plastic polymers. The second process is known as Material Extrusion. This uses a nozzle to push material through a die at a fixed cross-section. This is popular for manufacturing objects with complex shapes and orientations (All3Dp, 2020). The third process is VAT Photopolymerization. This is a more complex method that involves lowering a printing bed into a liquified photopolymer resin. An ultraviolet light is then used to cure the material into a solid state. This is mostly used for larger prints because the size of the printing bed is significantly larger than that of material jetting or binder jetting (All3Dp, 2020). The fourth process is sheet lamination. This process works by using sheets of material and ultrasonic lasers to weld ribbons of metal into a solid object. The next process, Direct Energy Deposition, uses laser-engineered net shaping. This is a highly complicated process that is most commonly used to add new material to an existing object that has been damaged. The sixth process is binder jetting, which uses a liquid binding agent to form objects on a printing bed (All3Dp, 2020).

The final process is known as powder bed fusion. This process fuses powdered material into a solid object by using a single focused laser or an electron beam. The focus of this MQP is laser powder bed fusion process. The first step in the overall process is to create a computer aided design to model the specifications of the print. That file is then sent to be loaded into the computer of the LPBF printer. Once the machine is setup and loaded with the powdered metal, the print is ready to begin. First, oxygen is expelled from the airtight chamber and argon gas is pumped in to ensure a controlled inert environment for the print. Then, a thin layer of powder (20 – 60 microns) is applied to the build region to begin. The laser beam selectively melts the powder layer as per the CAD model. After this, more powder is then dispensed on top of the previous layer and the laser melts the second layer as per the CAD model. This process of powder spreading, and selective melting is repeated until the part fabrication is complete. After fabrication, a brush or compressed air is used to clean away any remaining powders present on the finished part. The basic LPBF components can be seen in Fig. 1 and an overview of the steps is provided in Fig. 2.

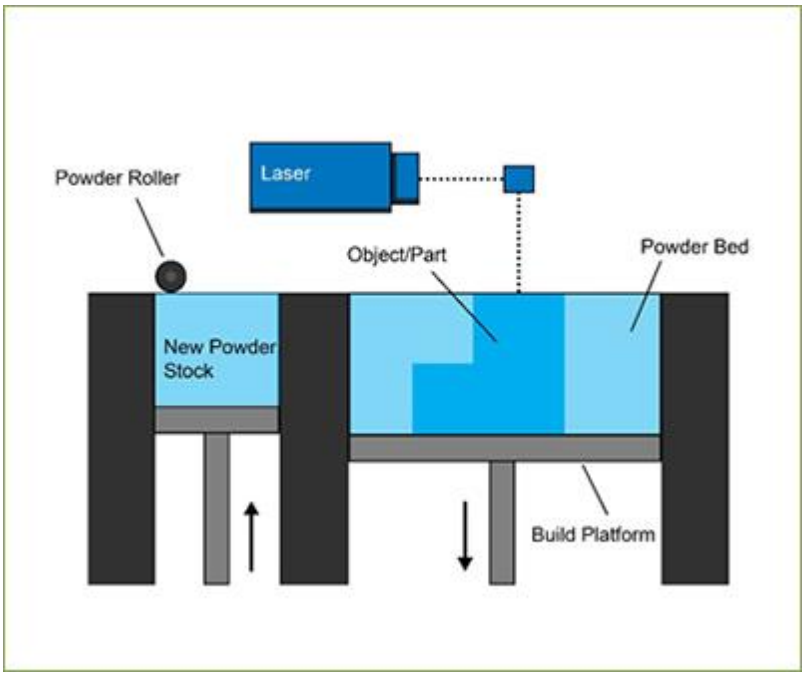

Figure 1: Schematic of a LPBF printer (Loughborough University)

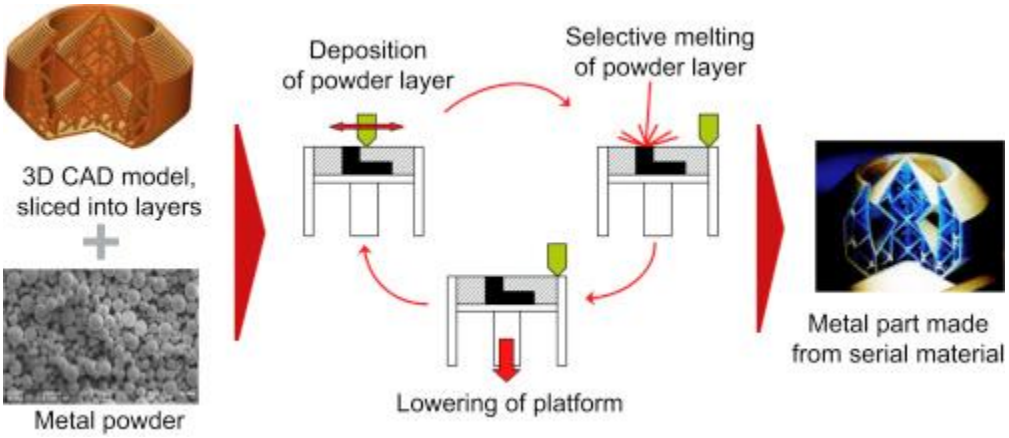

Figure 2: LPBF complete process (Loughborough University)

Some of the most common uses of the LPBF process are in the aerospace field because of the high strength and low weight prints that it can produce. LPBF also reduces the overall amount of parts in a system because it can combine elements from multiple different pieces. Another common use for LPBF is in the automotive field. The manufacturers of Bugatti are currently using the LPBF process to manufacturing brake calipers, and other fully functional parts for the automobiles. Frank Götzke, Head of New Technologies at Bugatti, commented on the brake caliper, saying: “Proof that additively produced metal components can cope with extreme strength, stiffness and temperature requirements at speeds of over 375 km/h with a braking force of 1.35g”. Audi also now uses LPBF to manufacture their engine water connectors for their W12 engine

which can be seen in Fig 3. The functional ability of LPBF parts are constantly being improved on as the technology continues to grow.

Figure 3: Water connector for Audi W12 Engine made by SLM Printer

2.2 Need for Economical Prototype

Purchasing a standard industrial grade selective laser melting LPBF machine today would cost anywhere from $500k - $1M depending on the features, required build dimensions, and other specs (Stevenson, 2017). This does not include the installation costs surrounding the implementation of the machine on a manufacturing floor, the procedural costs surrounding the proper training of operators, and material/maintenance costs. It is apparent that incorporating these machines into a company's manufacturing and prototyping department would require a hefty investment, and any kind of void to warranty would be detrimental to a consumer. This hinders the expansion of the LPBF industry because operators cannot experiment with the technology without jeopardizing significant assets.

Researchers have attempted to solve this problem through a couple methods. Firstly, computer modeling programs have been used to emulate material interactions with laser LPBF (Ma et al., 2015). An example of this process attempts to avoid the use of a physical mechanism all together by utilizing a finite element model to manipulate parameters individually. Others have attempted to build in-situ LPBF systems that have improved viewing features for optimal imaging and X-rays (Bidare et al., 2017). This was done to observe fundamental build processes and control strategies. While these options both yield useful results when attempting to learn about material interactions, there is no standardized method that allows for the wide-scale experimentation of the LPBF process.

2.3 Material Limitations

While there exists a variety of metal alloy powders that are available for use in standard machines, the LPBF industry faces many challenges with material limitations. LPBF requires powders to be within a particle size of 15-60 microns (Digital Alloys, 2019). It also requires particles to be of

specific morphologies to ensure consistent structural properties of the print. Special considerations in handling and storage of the powders must also be taken to prevent oxidization. This makes production of these powders expensive and difficult to access. Metal powder alloys available for commercial use in PBF processes are listed below in Table 1 (Rockwell Laser Industries, 2019).

Table 1: Compatible material list for PBF

	L-PBF	E-PBF
Titanium (Ti6Al4V, grades 2, 5)	✓	✓
Titanium Aluminide		✓
Cobalt Chrome (CoCr, CoCrMo, CoCrW)	✓	✓
Tool Steel (Maraging)	✓	
Stainless Steel (17-4, 15-5, 316L)	✓	
Inconel (625, 718, HX)	✓	✓
Aluminum (AlSi10Mg casting grade)	✓	
Copper (CuSn10, Bronze)	✓	✓
Tungsten	✓	
Precious Metals (Gold, Silver, Platinum)	✓	

While these strict particle requirements are in place to ensure quality, parts printed with LPBF machines still are highly variable in structural properties and material characteristics (Digital Alloys, 2019). Properties such as surface roughness, material strength, mechanical density, and more are often inconsistent from print to print. This limits the use of parts printed in LPBF machines significantly due to the unreliability in material properties. If these variable characteristics could be controlled, the uses and applications of LPBF would greatly increase.

2.4 Experimentation Limitations of LPBF Printers

With new research and experimentation, more materials could be used inside the LPBF chamber, allowing new industries to make use of this lean technology. In order to conduct testing on new materials and different technologies inside the printers, researchers would be required to manipulate expensive printer machines from companies that manufacture them. In many cases, any manipulation to critical components of the machine that affect its form and function will result in a breach in warranty and insurance on the machine. Since printers can reach up to the million-dollar range, this is just not feasible for many researchers as a failed machine component without customer service from the provider could render the printer useless. This problem in the AM metal printing industry is the reason why this project is critical to researchers going forward.

2.5 Gantry and Galvanometer Systems

One of the main challenges facing this project is the laser projection and movement system. In the commercial use of lasers with laser cutters, engravers, and printers, either a gantry system or a

galvanometer is used. In order to determine which system will work best for a prototype LPBF machine, the benefits and limitations of each must be discussed.

A gantry system, as seen in Fig. 4, is an xy plotter typically found in common laser engravers, laser cutters, and various AM machines. For a gantry system involving lasers, typically three mirrors are fixed in place at 45°. One mirror will direct the initial laser beam up along either the x or y axis depending on where the laser is positioned. A second mirror will sit fixed along one of the moving arms of the gantry system, moving with that arm. This mirror will deflect the beam onto the plotter mirror which will project the beam vertical onto the working surface. The plotter mirror will always be over the xy point of that job. Some advantages of a gantry system for a PBF machine includes a larger working platform. Typical gantry systems support a minimum working platform of 2”x2”, however, many are much larger. There is no real limit on the size of the working platform when using a gantry system. This system is also simplistic in comparison to the galvanometer. Fabrication of a gantry system is cheap, with few parts needing to be precisely aligned. When using a gantry system, machines are limited to slower moving laser positions as the physical plotter must move from point to point. Speeds will depend on the motors used, but to avoid overspending, a high-speed gantry system is unreasonable in a LPBF printer. This negative aspect is noted by Mirjam Knothe of the University of Applied Sciences in Aachen when an attempt was made to reduce LPBF machine costs by using a gantry system (Knothe, 2018). Additionally, inside a LPBF box, it is crucial to maintain a stable work environment so to not disturb the powdered metal that will be melted. A moving gantry plotter could easily disrupt the resting powder. These metal fragments will eventually affect the mechanical components of the system, leading to higher wear and tear that need maintenance (Cao, 2017). Now that the gantry system has been discussed in depth, the galvanometer will now be looked at.

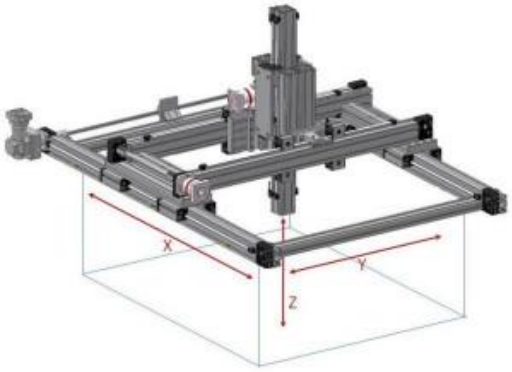

Figure 4: XYZ gantry system found in typical laser cutter (Macron Dynamics, Inc.)

A galvanometer, commonly referred to as a “galvo”, is a moving mirror technology in which small mirrors make angular adjustments to deflect a beam onto a corresponding xy point. Most galvanometers consist of two mirrors, two computer-controlled motors, and a lens. One mirror orients itself to correspond to an x coordinate, so this mirror will be called the x mirror. The second mirror will position the beam to the correct y coordinate; thus, it is the y mirror. Once the

laser beam is positioned to hit the correct xy point, an f-theta lens is required to focus the beam onto the working platform. Fig. 5 shows two schematics for a galvanometer design.

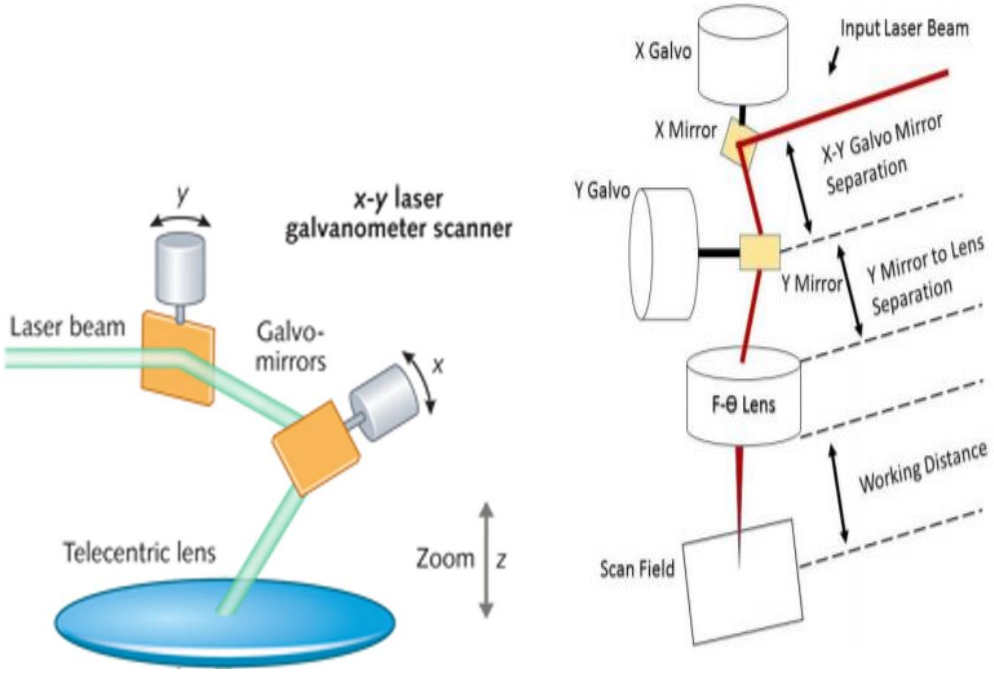

Figure 5: Galvanometer scanners schematics (Cao, 2017)

Galvanometers are computer controlled and have precise motors that can move smoothly and quickly to project the laser accurately. Galvanometer systems are more compact than the gantry system. Also, since laser light can be regarded as a massless tool (Chen) there are no forces acting on the laser and it can move from up to 10 to 60 times faster than a gantry system in a LPBF system (Chen). Galvanometers are known for their ability to swiftly scribe accurate text, bar codes, and various designs within a tight tolerance. Although the computer software is more complex than a gantry system, a typical PC computer is enough to control the movements of the motors. One of the main limitations of the galvanometer system is its limited working platform. Since the laser can only be deflected so much, most galvanometer LPBF machines can only have a working platform of around 18” x 18”. To increase the size of the working platform, multiple galvanometers must be used which increases cost and complexity.

After looking into both gantry and galvanometer systems for the prototype LPBF machine, the galvanometer system was chosen. The ideal speed for the laser movement inside the chamber is at least 1000 mm/s. This would be an unattainable goal with a gantry system working within the budget allowed. A galvanometer can easily deflect a beam to speeds exceeding the minimum needed. In regard to the galvanometer’s limited working platform, this prototype only needs a small working platform of 12”x12” for the experiments that will be conducted. To reduce spending and increase accuracy, the galvanometer will provide a compact yet more accurate means of

positioning the laser on the working platform. Now that the galvanometer system has been decided upon, an f-theta lenses must be chosen in order to correctly focus the beam.

2.6 F-Theta Lens

Once the laser beam has been deflected to reach the correct xy coordinate on the working platform, an f-theta lens must focus the beam so that it strikes the bed at around a 100 μm diameter. If the laser beam is defocused, the power density might not be sufficient to melt the powdered metal. Also, if the beam is focused too finely, the power density could be too high and the laser could easily penetrate too deep into the substrate. The energy input should melt the power layer and the layer underneath the current layer to ensure connectivity between layers (Bergman, 2016). An f-theta lens usually consists of two spherical lenses positioned on either the emitting side or the input side of the galvanometer. The two different positions of the f-theta lenses are known as pre-objective (emitting side) and post-objective (input side) (Chen). Although the actual laser beam quality will not change based on the f-theta lens orientation, most LPBF galvanometer systems use the pre-objective orientation of the f-theta lens, so the LPBF prototype box will use this orientation for simplicity in design. A drawing of the function of the pre objective f-theta lens is portrayed in Fig. 6 where the term "scanner" refers to the X and Y mirrors in the galvanometer:

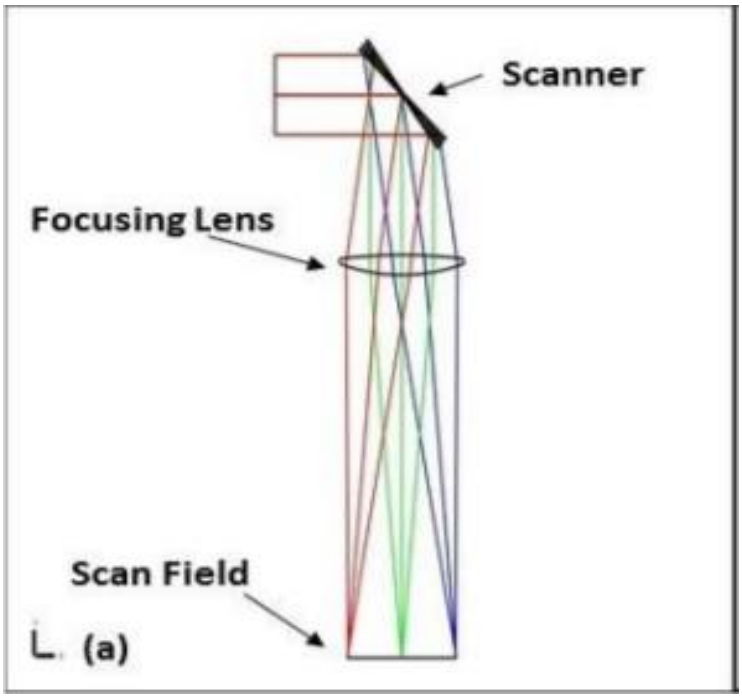

Figure 6: F-Theta lens pre-objective position (Chen)

2.7 Laser Basics

Lasers, an acronym for light amplification by stimulated emission of radiation, come in all different types, shapes, sizes and applications and are widely used in the ever-expanding technological world we live in today. Lasers are used in everything from toys, to the most advanced forms of additive manufacturing in industry today (Lawrence Livermore National Laboratory). Although not all lasers are the same, they all follow the basic principles that will be discussed.

Lasers work by emitting photons in an extremely directional and controlled manner, producing a narrow beam that can be focused to produce work on an object. All lasers contain a tube filled with a medium of atoms. These atoms will be excited by means of DC or AC current from an exterior power supply. When an atom is exited, it's electron will "jump" from its relaxed state orbit to a higher energy orbit. The excited electron will then quickly return to its relaxed state. In the process of returning to its original state, an electron must release some energy that it gained. This energy release is in the form of a photon which we see as visible light (or other forms of light that cannot be seen such as infrared light). This process is depicted in Fig. 7 below.

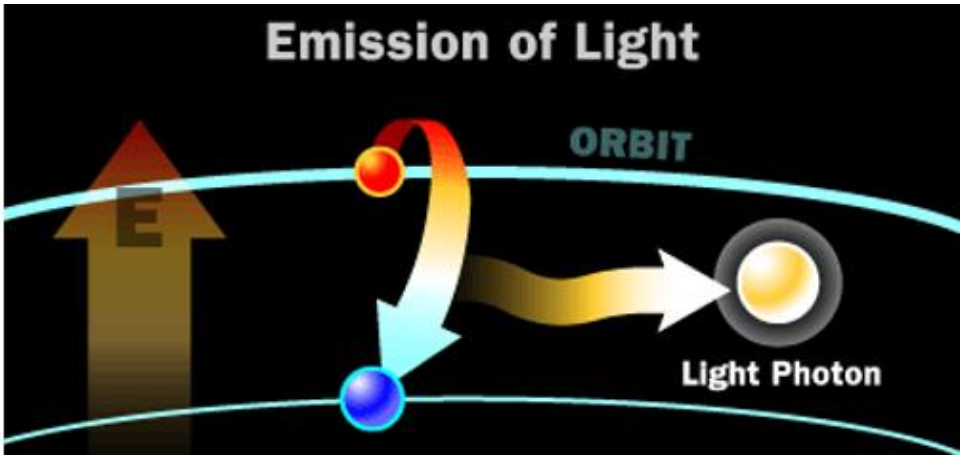

Figure 7: Emission of photons in laser medium tube (Spring, 2009)

Inside the laser medium tube, one excited electron that releases a photon energy will then excite other electrons near it. Soon, many electrons will be reaching higher energy orbits and emitting photons. In lasers, all the electrons inside the tube will release photons at the same wavelength, known as monochromatic light (Spring, 2009). This process of one photon exciting other electrons to release more photons of the same monochromatic light is called coherent or organized light release. This means that the photons move in step with each other, creating a continuous release of light. Because the photons are confined to the medium tube, the light becomes directional. The monochromatic, coherent, and directional aspects to the photon emissions in the laser medium tube make lasers different from other light emitting devices such as a flashlight or a lightbulb. Now that the medium tube has created organized light, mirrors inside the tube must work to increase photon emission and emit the laser in the form of a beam.

Lasers medium tubes contain mirrored surfaces on both ends. These mirrors will reflect the photon emissions within the tube to excite more and more electrons. Once the buildup of photons is sufficient, a beam is ready to be released. As long as a power source is applied, laser medium tubes will continue to produce photons at an extremely high rate. One of the tube's mirrors is a partial mirror, meaning it reflects some light but also allows light to pass through (Hecht, 2011). This output mirror is where the beam will be emitted from and can be seen the schematic depicted below. A detailed schematic of what happens inside a laser medium tube can be seen below in Fig. 8.

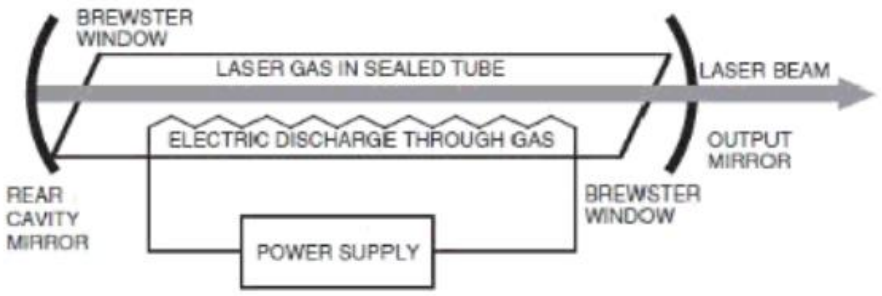

Figure 8: Mirror schematic inside laser (Hecht, 2011)

Laser beams can be created from solid-state lasers, gas lasers, excimer lasers, and semiconductor lasers, however, most lasers inside industrial machines use gas lasers or solid-state lasers. CO_2 lasers, the earliest form of gas lasers, emits a high energy infrared beam ranging in wavelength from 9.0 to 11.0 μm (with10.6 μm being the typical wavelength for AM) that contains a great deal of energy, capable of cutting steal (Lee, 2011). CO_2lasers, developed in 1964, consist of the same mirror, tube, power source components as described above using carbon dioxide as the medium inside the tube. In today's application, CO_2lasers are mainly used to cut, drill, and weld metal parts in a variety of applications and machines. With power from the beam reaching up to 20 kW, CO_2lasers are perfectly suited to be main laser used within machines that need to cut, drill or weld organic materials, as well as metals. Due to the high energy produced by the photons, many CO_2lasers contain water cooling tubes inside the medium tube to prevent overheating and result in a very efficient laser with minimum maintenance to keep operational. The main limitation of the CO_2laser is that it is not capable of fiber optic delivery because fiber optics cannot support the wavelength range that these lasers produce (Lee, 2011). An example of a CO_2laser connected to a scanning system can be seen in Fig. 9.

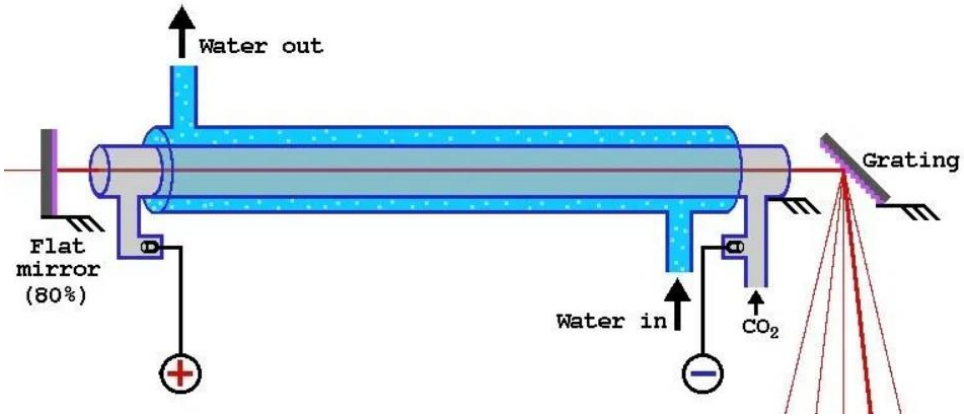

Figure 9: CO_2 laser schematic including galvanometer setup (Lee, 2011)

Another form of lasers more commonly used in LPBF printers are the Nd:YAG solid-state laser. These lasers use Neodymium (Nd) diffused in a crystal that is composed of yttrium aluminum garnet to produce a light beam in a similar way to how the laser medium tube works

with a gas laser. Nd:YAG lasers produce a wavelength 10 times smaller than a CO_2 laser, around 1.64 micrometers. This near infrared beam is great at engraving, welding, and cutting through metals at a faster speed than CO_2 lasers. This improved capability of cutting metal is due to the beam's smaller wavelength, as reflective metal particles prevent penetration in larger wavelengths, such as a CO_2 laser. The Nd:YAG laser is also capable of fiber optic delivery, which is important in the scope of this project and will be discussed later in the report. These characteristics of the Nd:YAG laser make it the most popular laser used within LPBF systems.

2.8 Safety Considerations

When working with a LPBF system, several safety concerns must be considered. To ensure that a working model will be safe for use, an extensive review of the potential hazards surrounding the system is required. The two major areas of potential safety hazards to focus on for a selective laser melting LPBF system involve the thermal component (laser) and the metal powders.

2.8.1 Laser Safety

Lasers can produce a wide range of high-density photon wavelengths (200 nm – 1000 µm) that could cause damage to the skin or eyes if not handled properly (Noir, 2017). The most dangerous aspect of a photon laser beam involves direct or diffracted exposure into the user's eye. Depending on the wavelength and intensity of the beam, permanent retina damage could occur, which would render the user blind. Roughly 15 retinal eye injuries are reported due to industrial grade lasers each year (Mainster, 2019). While this may not seem like a lot, this does not touch on the other eye injuries that effect the cornea and lenses, as well as the many skin injuries that could be caused by high beam-intensity lasers. Table 2 provides information on the potential harm specific wavelengths of laser beams could cause.

Table 2: Overview of hazards associated with laser wavelengths (Oregon State University, 2019)

Photobiological Spectral Domain	Eye	Skin
Ultraviolet C (200 nm - 280 nm)	Photokeratitis	Erythema (sunburn) Skin Cancer Accelerated skin aging
Ultraviolet B (280 nm - 315 nm)	Photokeratitis	Increased pigmentation
Ultraviolet A (315 nm - 400 nm)	Photochemical cataract	Pigment darkening Skin burn
Visible (400 nm - 780 nm)	Photochemical and thermal retinal injury	Pigment darkening Photosenstive reactions Skin burn
Infrared A (780 nm - 1400 nm)	Cataract and retinal burn	Skin burn
Infrared B (1.4µm - 3.0 µm)	Corneal burn, aqueous flare, cataract	Skin burn
Infrared C (3.0 µm - 1000 µm)	Corneal burn only	Skin burn

To understand the potential risks of a certain laser in use, there exists a standard laser classification system that emphasizes the risk associated with a given laser wavelength and power output. These laser classifications are shown in Table 3.

Table 3: Overview of laser classes (Oregon State University, 2019)

Class	Type of lasers	Meaning	Relationship to MPE	Hazard Area	Typical AEL for CW Lasers
Class 1	Very low power lasers or encapsulated lasers	Safe	MPEs are not exceeded, even for long exposure duration (either 100 seconds or 30000 seconds), even with the use of optical instruments	No hazard area (NOHA)	40 µW for blue
Class 1M	Very low power lasers; either collimated with large beam diameter or highly divergent	Safe for the naked eye, potentially hazardous when optical instruments** are used	MPEs are not exceeded for the naked eye, even for long exposure durations, but maybe exceeded with the use of optical instruments**	No hazard area for the naked eye, but hazard area for the use of optical instruments** (extended NOHA)	Same as Class 1, distinction with measurement requirements
Class 2	Visible low power lasers	Safe for unintended exposure, prolonged staring should be avoided	Blink reflex limits exposure duration to nominally 0.25 seconds. MPE for 0.25 seconds not exceeded, even with the use of optical instruments.	No hazard area when based on unintended exposure (0.25 seconds exposure duration)	1 mW
Class 2M	Visible low power lasers; either collimated with large beam diameter or highly divergent	Same as Class 2, but potentially hazardous when optical instruments** are used	MPE for 0.25 seconds not exceeded for the naked eye, but maybe exceeded with the use of optical instruments**	No hazard area for the naked eye when based on accidental exposure (0.25 seconds exposure duration), but hazard area for the use of optical instruments** (extended NOHA)	Same as Class 2, distinction with measurement requirements
Class 3R	Low power lasers	Safe when handled carefully. Only small hazard potential for accidental exposure	MPE with naked eye and optical instruments may be exceeded up to 5 times	5 times the limit of Class 1 in UV and IR, and 5 times the limit for Class 2 in visible, i.e. 5 mW	5 times the limit of Class 1 in UV and IR, and 5 times the limit for Class 2 in visible, i.e. 5 mW
Class 3B	Medium power lasers	Hazardous when eye is exposed. Wear Eye Protection within NOHA. Usually no hazard to the skin. Diffuse reflections usually safe	Ocular MPE with naked eye and optical instruments may be exceeded more than 5 times. Skin MPE usually not exceeded.	Hazard area for the eye (NOHA), no hazard area for the skin	500 mW
Class 4	High power lasers	Hazardous to eye and skin, also diffuse reflection may be hazardous. Protect Eye and skin. Fire hazard.	Ocular and skin MPE exceeded, diffuse reflections exceed ocular MPE	Hazard area for the eye and skin, hazard area for diffuse reflections	No limit

All LPBF systems involve the use of a Class 4 laser (Slotwinski, 2017). This means that the laser could cause severe damage from direct or indirect exposure to the skin or eyes. When the laser beam hits an object, a portion of the photons are absorbed into the material, another portion is transmitted through the materials, while the rest is reflected and scattered off into surrounding objects. Therefore, laser equipment is often constructed with dark-colored materials so that most of the photons are absorbed upon contact.

To avoid injury from diffracted laser beams, LPBF systems are often housed with minimal windows for viewing, and the user is required to wear protective eye gear that prevents the laser beam from transmitting through (Rockwell Laser Industries, 2019). It is important to understand what kind of eye wear and viewing windows prevent the proper wavelength of photons emitted from the laser to ensure that the user is protected. Selecting appropriate eye wear involves choosing glasses that reflect that wavelength range that the given laser emits (in nanometers) and the optical density. Optical density is defined as "…a measure of the attenuation of energy passing through a

filter. The higher the OD value, the higher the attenuation and the greater the protection level. In other words, OD is a measure of the laser energy that will pass through a filter." (Noir, 2019). If the chosen eye wear does not reflect the wavelength that the laser emits, the beam will pass right through the glasses. Similarly, if the optical density of the glasses is not high enough, the energy from the beam will still transmit through the glasses even though it is within the proper wavelength range. Standard viewing windows for class 4 lasers operate in a similar manner to protective eyewear where specific types will protect against certain wavelengths and power densities.

2.8.2 Metal Powder Safety

The metal alloy powders used in LPBF processes introduce a variety of safety hazards as well, which include combustions hazards, skin irritation, and potential for inhalation (Digital Alloys, 2017). The kinds of metal powders used in LPBF range in particle size, metallurgy, and material characteristics, which means that the protocol when handling a certain material can differ greatly depending on what the material is. Because of this, there is no standard safety procedure for how to handle these materials in LPBF processes. However, Safety Data Sheets exist for every kind of metal alloy powder used in LPBF, and it is the operator's responsibility to understand the information on these sheets prior to handling the substances. A level of understanding about the material being worked with as well as the environment the user is working in is crucial to minimize hazards as well (Slotwinski, 2017).

The potential for combustion must always be addressed by replacing the oxygen in the build chamber with an inert gas. This is because the laser beam produces a large amount of thermal energy in a small area, which could create flames if exposed to oxygen. Skin irritation is less of an immediate danger to the user but must be considered when designing the chamber and handling the powder prior to use. Inhalation of the metal powders is a greater danger due to the potential for powder to reside in the operator's respiratory tract during pre and post-processing (Beer, 2018).

A study that investigated the respiratory hazards associated with three titanium-based powders commonly used in LPBF found that the safety data sheets for the powders did not provide ample safety information on the respiratory effects or the proper procedure when the operator has potentially inhaled the substance (Preez, 2019). This means that handling these powders pose a heightened risk and should be treated with extreme care.

3.0 Design

Development of the LPBF system requires careful consideration for mechanical design of localized components, as well as the entire assembly. Analysis of the system was broken down into subgroups based on key physical features. These subgroups were then brought together in a functional CAD model to allow for analysis and prototyping preparation. To properly address the key features within the design and fabrication of the LPBF system, objectives were identified:

1. Develop an airtight, structurally sound frame to house a bed leveling system, powder roller, and mirror galvanometer system.
2. Develop a movable bed system capable of micron-increment leveling and placement for substrates of varying dimensions.
3. Develop a door that provides an airtight seal, viewing window, and removable components.

4. Develop a mirror x-y scanner system to direct the laser beam in a desired motion.

3.1 Design Requirements

Following the identification of the objectives for this project, it was crucial to clearly state the requirements that must be incorporated into the design to successfully accomplish this objective. These requirements drove ideation of initial design concepts for iterative development. Below is a bulleted list of these requirements:

Robust chamber frame

The chamber which will house all components for the project must be made from a strong, abrasion resistant material. Experimentation that will occur within this chamber could subject the structural materials to a wide range of thermal and mechanical forces. Since it is not practical to identify these possible forces, the material used must subjectively be incredibly strong, abrasion resistant, have a high service temperature, and have a long fatigue life.

Adjustable bed plate

The prototype must contain a 12” x 12” bed plate that is capable of being leveled to a fine degree of measurement. The system is planned to be used with a multitude of experimental substrates and powders of varying dimensions. Because of this, the bed plate must accommodate fixtures for placement of these substrates. The maximum substrate size to be placed on the bed plate will be ~10” x 10” with a minimum size of ~2” x 2”.

Bed-leveling system for consistent power dispersion

The design must feature a leveling system to ensure that the build plate is parallel to the ground and the powder will remain in place during melting. This leveling system must also be capable of moving the bed up and down to a degree of microns for placement of new layers of powder. It is essential that the powder layers are dispersed evenly over the substrate to ensure consistent melting behavior.

Adaptable gas flow inlet/outlet ports

LPBF requires an inert gas such as argon to be present within the chamber during fusion to minimize any unwanted material defects that could occur from the presence of oxygen in the air (Brandt, 2017). This also will mitigate fire hazards as argon and other inert gasses do not combust with the absence of oxygen. Furthermore, this reduces oxidization of the alloy powder to achieve homogeneity of mechanical properties within the structure. Due to time and budgeting constraints, computational modeling of the fluid flow within the chamber does not fit within the scope of this project. To accommodate for various inlet and outlet gas flow arrangements, an adaptable port must be implemented into the design of the frame.

Space for a powder bed roller for even distribution of powder

Most LPBF systems require a series of electrical-mechanical and hydraulic components to properly disburse metallic powder across the build plate and roll it on evenly (Digital Alloy, 2017). However, our chamber prototype will only require the use of a few layers of powder to be dispersed onto a build plate to be able to properly study the interaction with the laser. This means that our design will not require the use of hydraulic pistons for bed movement, or an automatic powder

roller for adding additional layers. However, it will be important to provide space in our chamber design to allow for retrofitting of the powder roller in the future.

A functioning galvanometer to position the laser in desired locations

The galvanometer must meet the required travel speed of around 1000 mm/s. Most commercial grade galvanometers start at a minimum price of around 300 dollars. Since this is not within the budget of the project, a prototype galvanometer must be fabricated. The galvanometer must be able to connect to a computer that can interpret G-code to the mirrors to project the beam onto the correct location.

Laser-diode for proof-of-concept

Typically, LPBF systems use a high wattage Nd:YAG laser that can produce high power-density beams that will fuse the metallic particles together. Since this would require money outside of the budget constraint, a diode laser will first be used within the galvanometer system to show proof—of-concept. This laser will be low wattage and will not be capable of cutting or fusing together metallic powder. The galvanometer must be designed so that a Nd:YAG laser can be retrofitted for later use.

F-Theta lens

This type of lens is used to focus a laser beam onto a desired point. These lenses ensure that even when the laser beam deflects in the x or y direction, a consistent spot size is maintained to focus energy where it needs to be. An F-theta lens is out of the budget for this project; however, a lens will be selected for future purchase based on the distance the galvanometer will be positioned above the bed plate. Additionally, a hole on the underside of the galvanometer where the laser beam emits from will be tolerance to fit the F-theta lens required for this design so it can retrofit in the future.

Laser-safe viewing windows

It is necessary when using a class IV laser that the laser does not have the ability to cause harm to anyone or anything. Since the goal of this LPBF system is to conduct experimental trials, it is essential that the user can see inside the chamber. This means laser safe viewing windows must be installed on all sides that are intended to be see through. This includes all sides besides the base of the chamber and the steel side which will house the gas ports. Laser safe viewing windows cost hundreds of dollars per windowpane to purchase at the size this chamber would require. Since this would result in going over budget, an alternate solution for the laser safe viewing glasses must be determined to meet budget requirements.

3.2 Design Constraints

With the project objective and requirements established, the constraints surrounding the design needed to be identified as well. These constraints allowed the team to develop a functional design for practical use while considering variables that effect the fabrication and eventual operation of the system. Below is a list of these constraints:

Budget of $750

Standard budgeting protocols for Major Qualifying Projects (MQPs) at WPI dictate that an allowance of $250 is given per member of an MQP team. This project followed this protocol which gave the team a final budget of $750 (three team members).

Retrofittability of expensive components

It is important to note that the fabrication of a fully functional LPBF system requires the implementation of many high-cost components such as a 400W Nd:YAG laser, laser-safe viewing windows, and beryllium coated mirrors with 99% reflectivity. Incorporating these components into the fabrication of the design exceeds the budget for this project. To account for this, affordable replacements for the components must be implemented to act as placeholders for the real ones. The design must consider the retrofit-ability of these high-cost components to ensure smooth replacement. A complete table of the components to be retrofitted can be seen in Table 4.

Table 4: Current Vs Final component list

Current Component	**Final Component**	**Means of Retrofit**
Acrylic Sheet	Laser-safe viewing window (1064 nm wavelength / 5+ optical density)	Glass features 6 through holes along perimeter. Fastened to compressive rubber lining via steel screws and washers. Can easily be removed for replacement with laser-safe glass.
Laser Diode 5mW	400 W Nd:YAG Laser / Collimator / Fiber optic Cable	Nd:YAG laser will have a fiber optic cable that feeds into a port on the backplate of the chamber. The galvanometer system will direct the laser beam in the X and Y directions on the build plate. The F-Theta lens will focus the beam to the desirable spot size normal to the build plate.
Glass mirror circle	Beryllium Coated galvanometer mirror	The stepper motors feature 3D-printed slots on their shafts for easy replacement of mirrors.
Vacant space for powder roller	PBF powder roller	Design for implementing powder roller is to be completed in further projects. Empty space is ample for accommodation of powder roller (~ 2 ft^2)

Manufacturing resources available at WPI's campus

A major design constraint of this project is to design the LPBF system for feasible fabrication using the manufacturing resources available on WPI's campus. WPI features a variety of manufacturing tools and equipment which include:

- CNC mini mills and lathes
- 3D polymer printers
- Laser-cutter
- Waterjet cutter

- Welding shop
- Metal and wood hand tools
- Power tools
- Solder stations
- Hot-wire cutters

3.3 Initial Designs

In order to maintain a level working bed platform inside the LPBF system, the bed plate will be separate from the box itself. The bed platform will be mounted on fine thread screws that can be easily manipulated to keep the bed at a level position. A small level will be installed onto the working bed platform so users can visually check that the bed is level before beginning testing with the LPBF system. Also, it is important that the entire LPBF system frame itself is level on whatever platform it rests on. This will be accounted for with 3D printed stands that are screwed into the base of the box. The stands can be twisted on the threads to produce fine increments of height to a certain side of the box in case the platform is not on a perfectly level surface. An initial hand drawn design of the LPBF chamber can be seen in Figures 10-12.

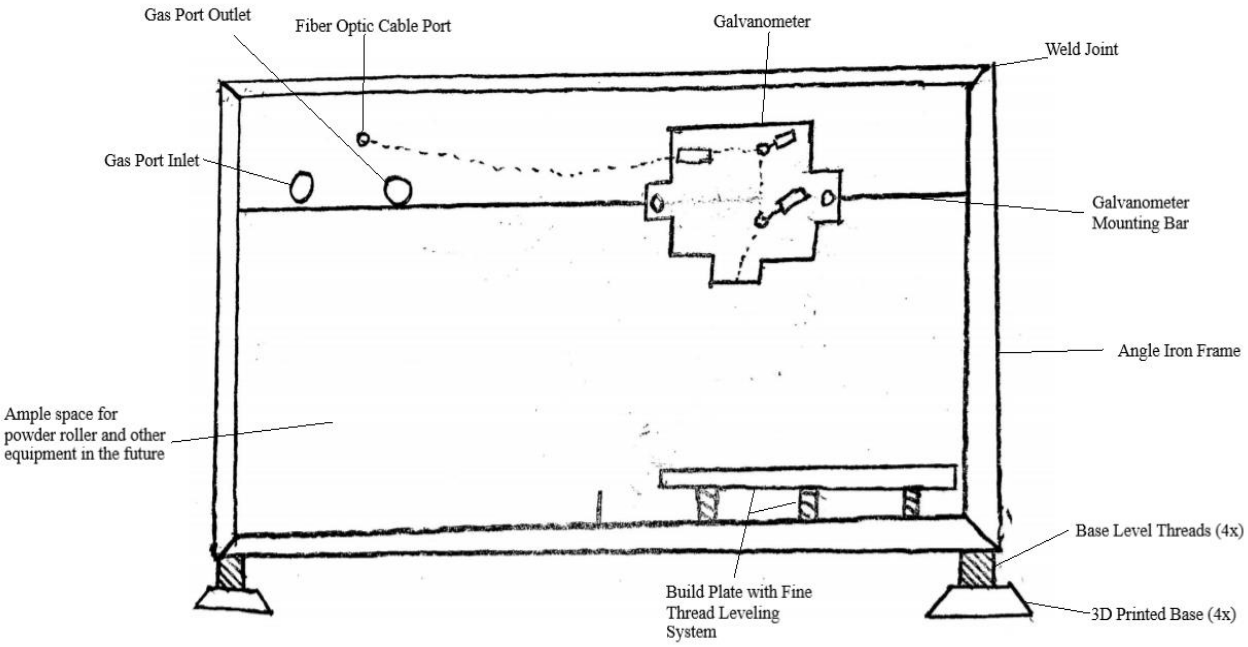

Figure 10: Front section view of LPBF hand drawing

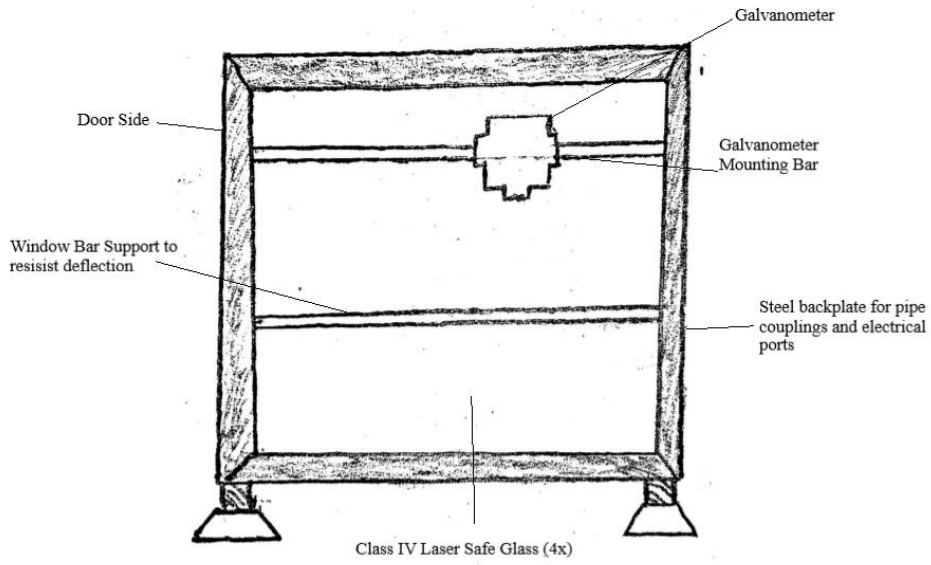

Figure 11: Side view of LPBF system hand drawing

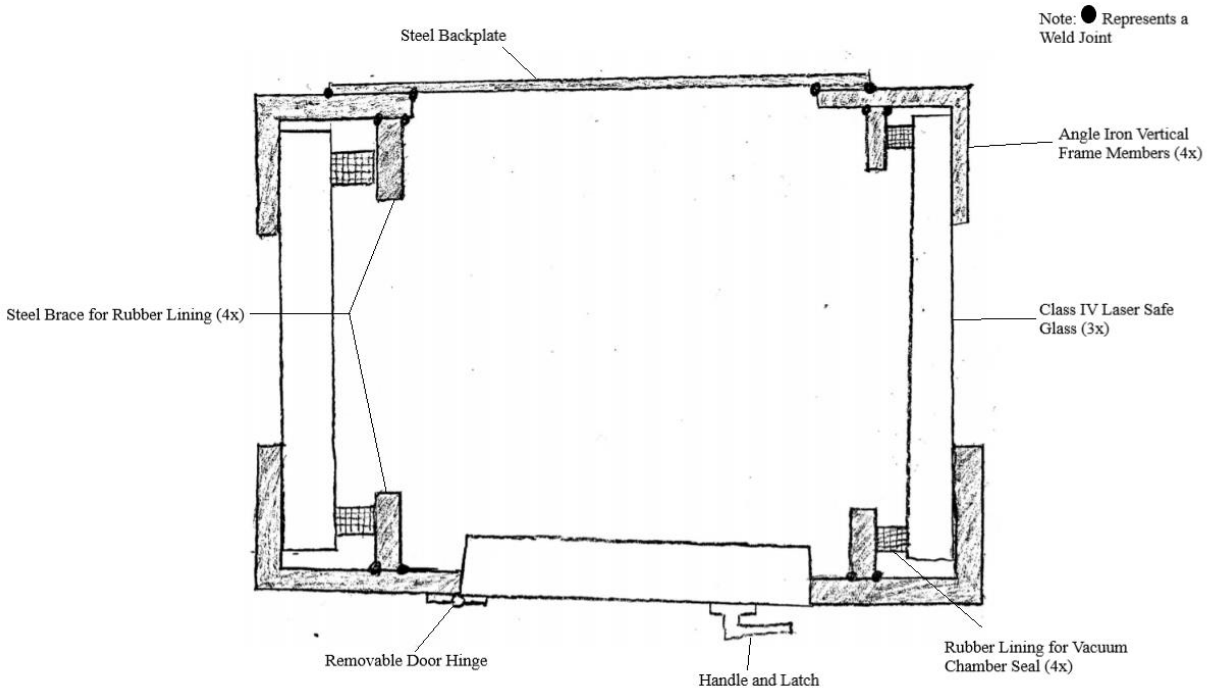

Figure 12: Top view of steel structure hand drawing

To make the chamber airtight and reliable for experimentation, the support structure must be strong and durable. To satisfy this requirement, the frame of the chamber will be constructed out of steel. This material will allow for a strong frame that will be weldable. Because of this, material analysis must be carefully considered in design as to not employ fabrication techniques on potentially hazardous materials (i.e. Welding zinc-coated steel).

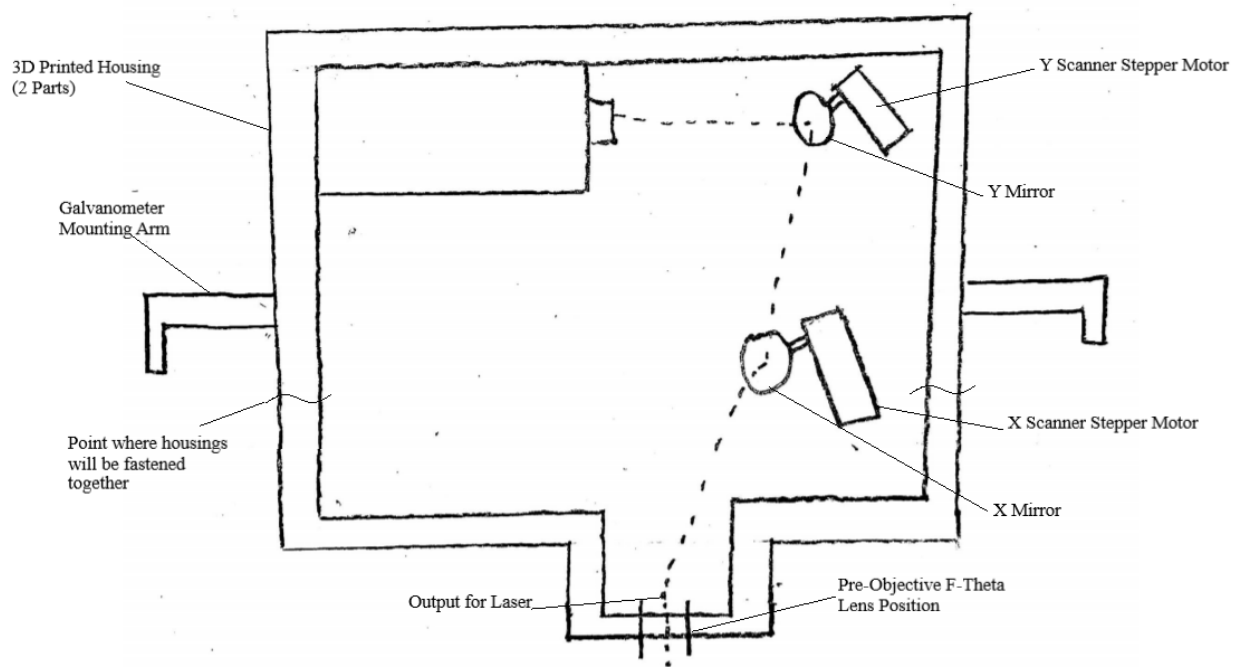

Figure 13: Galvanometer housing hand drawing

To create a galvanometer system that is fast, precise and able to be retrofitted with a Nd:YAG laser, an initial prototype will be developed and fine-tuned. The prototype must be created with cheaper material to meet budget requirements so it will not consist of the high-quality mirrors and stepper motors that commercial grade galvanometers possess. The prototype will consist of smaller scale stepper motors that can be computer controlled. The arms of the stepper motor will be able to be removed and a new arm will be designed that will be capable of holding mirrors that deflect a diode laser. The mirrors that are needed to deflect a diode laser are extremely cheap and will be used in testing the prototype. This is beneficial because when the Nd:YAG laser is retrofitted, new mirrors will be easily installed into the galvanometer that can handle higher energy laser beams. The prototype will contain the diode laser inside the galvanometer housing due to its small size and can be retrofitted with the correct Nd:YAG laser using fiberoptic cables. The entire galvanometer will be encased within a 3D printed housing that will be mounted inside the chamber. At the output of the galvanometer will be a circular opening where the F-theta lens will be positioned. Due to budgeting, an F-theta lens may not be implemented into this system, however, with the design of the housing of the galvanometer, an f-theta lens can be implemented in the future. The galvanometer will be positioned above the working platform on positioning bars that will run the length of the LPBF system. Initial hand drawn designs for the galvanometer system can be seen in Figures 13-15.

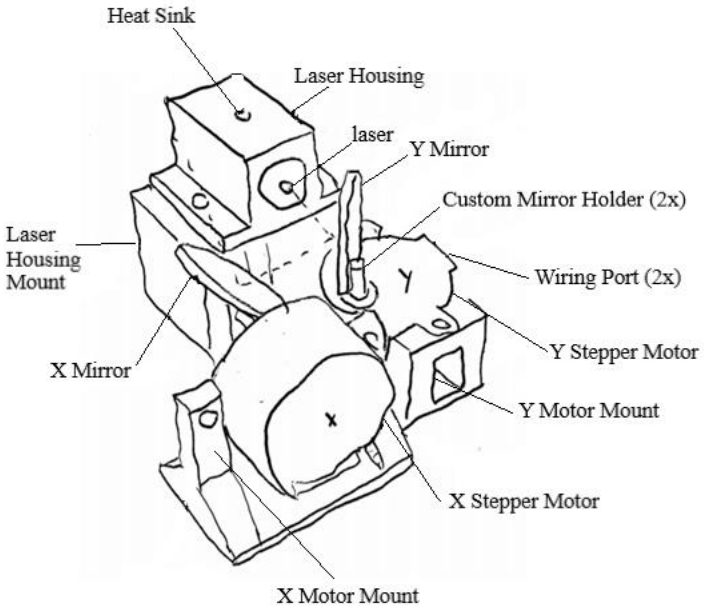

Figure 14: Isometric view of galvanometer mirror scanning system

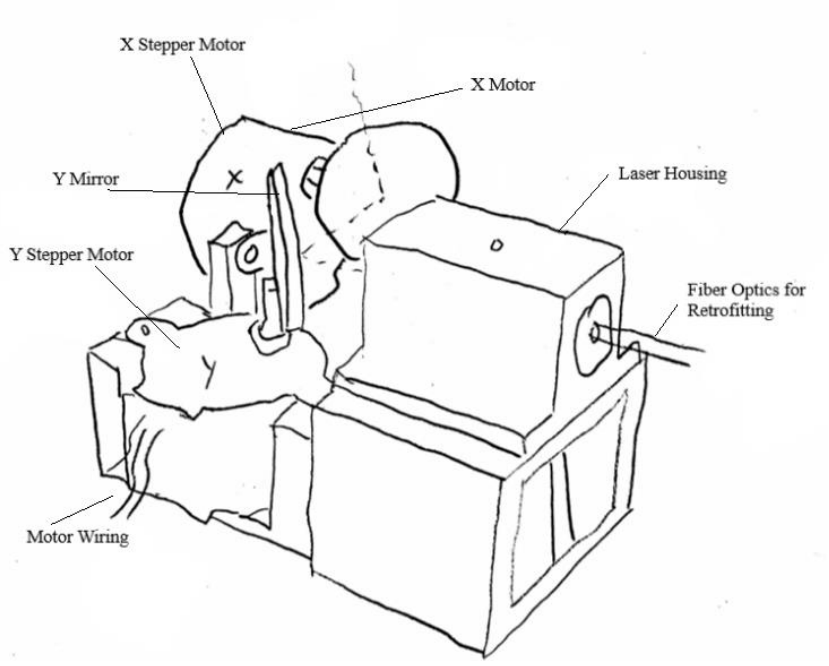

Figure 15: Additional view of galvanometer mirror scanning system

3.4 Galvanometer System Design

3.4.1 Initial Design

A mirror galvanometer is an electromechanical instrument dating back to the 1820's that senses an electric current by deflecting a beam of light with a mirror. Today, most mirror galvanometers are used in laser devices, deflecting these massless beams to sets coordinates in order to create, cut, and weld metals parts. Mirror galvanometer systems are found in laser powder bed fusion printers as they are accurate, fast, and compact. Mirror galvanometer systems for purchase range from $100-$1000 dollars. Any cheap galvanometer system for purchase uses standard mirrors that are fixed in place. In order to deflect a high-powered laser required for an LPBF printer, beryllium-coated mirrors with a reflectivity of ~99% are required. These galvanometers are much more expensive and out of the budget for this project. To compensate for this, a system that functions like a galvanometer will be fabricated.

The galvanometer system designed for this project will be created to draw various shapes onto a working bed platform. The system will be capable of deflecting any type of laser as the housing was designed specifically for retrofitting with more expensive equipment in the future. For prototyping and budgeting purposes, the galvanometer system was created using a diode laser and standard 1-inch diameter mirrors. Instead of using galvanometer motors, stepper motors were implemented, and the mirrors will be fixed to these motors. This system will use two mirrors, one for x direction and one for y direction. A detailed CAD model of the design can be seen below in Fig. 16.

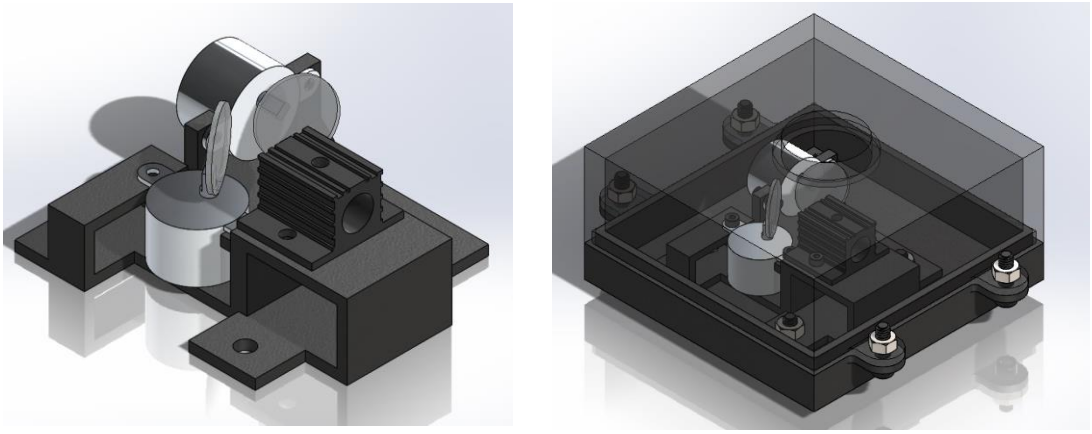

Figure 16: Galvanometer CAD model with housing

The galvanometer system will be mounted (as seen in picture above) and housed inside a 3D printed housing to keep out dirt and debris. The housing chamber will be in two parts. The top housing will secure the galvanometer system with nuts and bolts. The bottom side of the housing will have a port for a Thorlabs' FTH160-1064-M39 f-theta lens. The decision to 3D print the housing for the galvanometer system was made because it will result in an affordable system that has the capabilities of a regular galvanometer. Also, if any future adaptations need to be made to the design of the galvanometer, a new part can be quickly and affordably produced in-house at WPI.

The major downside to a 3D printed housing was the material's ability to hold shape under high heat. The ND:YAG laser can create hot temperatures inside the housing. To dissipate heat, a heatsink will be mounted on top of an aluminum laser housing. In addition, material analysis of 3D printed materials available to our group was conducted to choose the best option. A Pugh matrix was used to determine the best fit for this system and can be seen in Table 5.

Table 5: Pugh Matrix for 3D printer material

		Alternatives						
Criteria	Baseline	PLA	TPU	PC	ABS		Totals	Rank
Stength above 60 mPa	0	+	+	+	−		2	1
Stiffness	0	+	−	0	+		1	2
Can operate in Temps over 60C	0	−	0	+	+		1	2
Abrasion Resistance	0	−	0	+	+		1	2
Ease of Printing with	0	+	−	0	+		1	2
Cheap	0	+	−	−	+		0	9
	0						0	
	0						0	
	0						0	
	Totals	2	-2	2	4			
	Rank	3	4	2	1			

Upon completing the Pugh matrix, ABS is found to be the best option. The overall strength of the material is not as critical to this set up as is heat resistance. ABS can maintain its shape to temperatures up to 100 ºC. With the laser only on for a few layered experiments within the chamber, the ABS housing will be able to maintain its form and function under the heat produced by the laser.

3.4.2 Final Design of Galvanometer

After the first iteration of the galvanometer was completed, a few issues came to light that needed correction. First, many of the small screw holes that will mount the laser, the motors, and the baseplate were in areas that made it virtually impossible to attach a nut to the screw. The spaces they were in left little room for the user to fit their finger or a wrench underneath to fasten a screw to the nut. This was especially an issue under the x motor. To account for this, the design of the mounting shelves was adjusted so that inserting a nut under the mounting hole would be much easier. This can be seen below in Fig. 17.

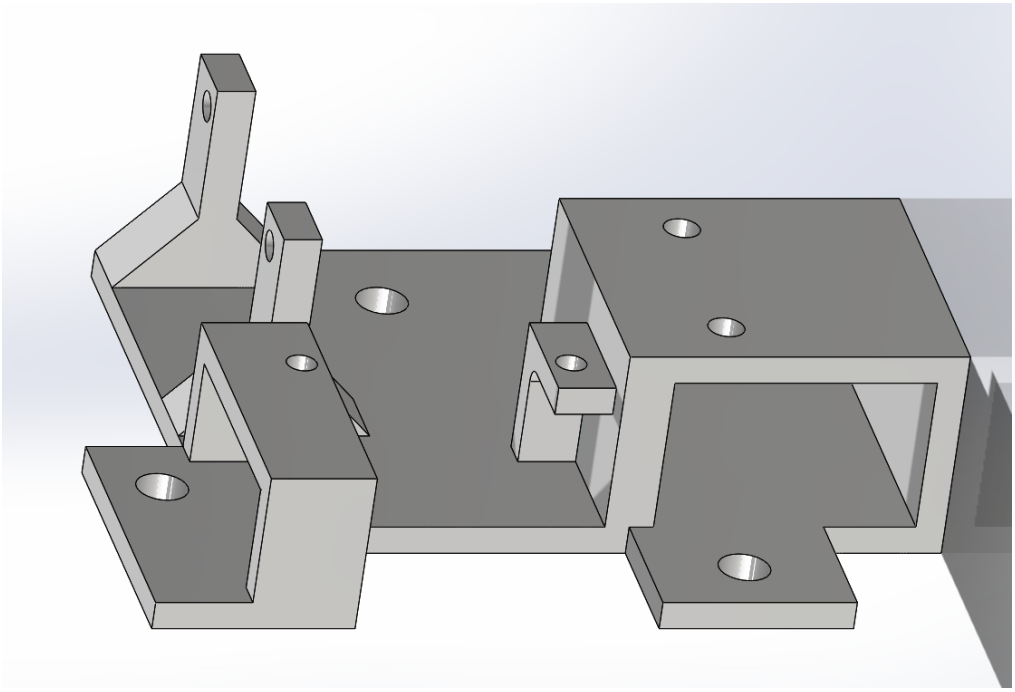

Figure 17: Galvanometer baseplate design

The next design change of the galvanometer system allowed for more space within the housing. Since a compact design for this galvanometer system is not crucial to the project, the housing for the galvanometer was expanded from a 4 inch x 4 inch housing to a 6 inch x 6 inch housing. It was noticed that after the first design was complete, there was no room for the copious amounts of wiring inside the housing. By expanding the housing as well as expanding the shelf for the laser mount, wiring would be able to be neatly organized within the housing.

The last change made was including output holes on the sides of the housing for the wires to leave from. Since the purpose of the galvanometer housing is to keep out dirt and debris from the sensitive electrical components, small holes were placed by the Y axis motor and behind the laser. This will allow for x axis motor, the y axis motor, and both snap switches' wires to be bundled up leave through one hole. The other output hole behind the laser was oversized to allow for the diode laser's wiring to leave through it but also allow for the thicker fiber optic cable of the Nd:YAG laser to be implemented in the future. These design changes, and the final version of the galvanometer can be seen below in Fig. 18.

Figure 18: Galvanometer system with housing

3.4.3 Electrical Set-up for the Galvanometer

Once the galvanometer has been assembled, the electrical components must be correctly configured. A Nano ATmega328 Micro-controller board for Arduino is positioned onto a solderless breadboard for the initial design. In the final version, the galvanometer will be connected to an Arduino Uno micro-controller board that will have more input pins to accommodate other electrical components in the system. The x and y 5-volt stepper motors are connected to a ULN2003 Driver board for Arduino. Both x and y driver boards are then wired to the micro-controller on the breadboard. Since these stepper motors do not track and record their position, snap switches will be implemented to home the motors each time they run. This process is very similar to how traditional plastic 3D printers track their position while printing. The snap switches will be connected to ground to ensure the stepper motors stop and return to their correct working position each time a program is run. The user will have the ability to quickly change this home setting within the code to correct for any misalignment in the laser. To power the motors, a micro USB will connect to any PC that can support Arduino C++ code. Since these motors can run at 5V, the PC alone can supply enough power, however, in the final version, this will be different as other components must run at a higher voltage. A schematic of the electrical wiring can be seen below in Fig. 19.

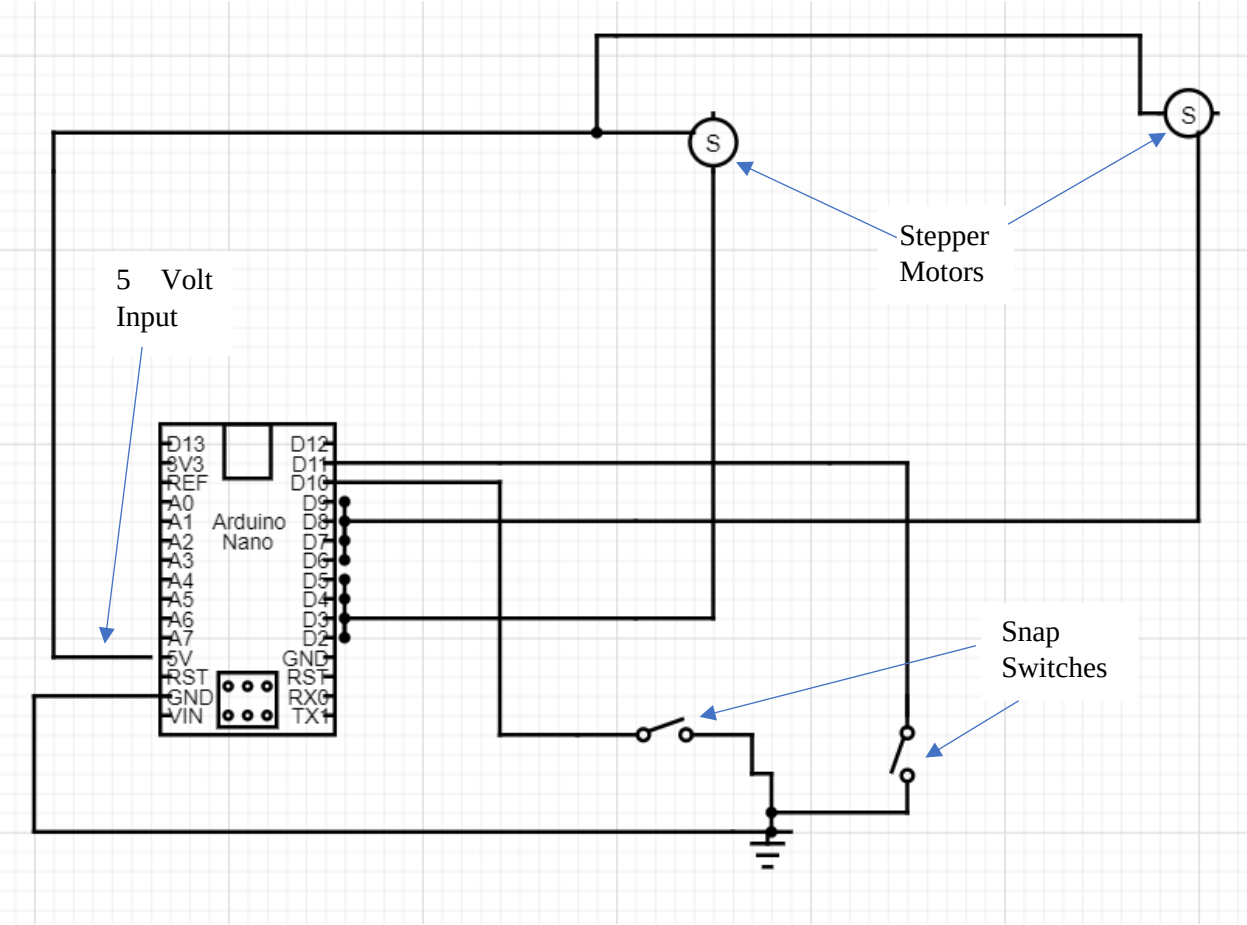

Figure 19: Electrical wiring schematic for Galvanometer

Lastly, the initial prototype will use a 650nm 3V Red laser module diode. This laser will stand as a visual representation of how the galvanometer system will work when the Nd:YAG laser is purchased and implemented. The laser will be powered by connecting its power and ground pins along the power and ground rails of the breadboard.

3.5 Chamber Design

In order to design a LPBF chamber that meets the requirements of this project, multiple ideas were presented and investigated. To ensure the chamber maintained a structurally sound body, welding the box out of steel was decided upon. Steel angle iron and steel rectangular tubes were the two structural materials discussed. Additionally, the chamber needs as many viewing windows as possible for experimentation purposes. The windows, which cover four sides of the system, needs to be sealed into place to minimize any argon leaking out. Placing the windows on either the inside or outside of the structural frame would greatly affect many aspects of manufacturing this chamber.

The first design iteration of a chamber with a welded angle iron frame and windows slotted inside the frame was modeled and can be seen in Fig. 20. This chamber was designed to incorporate a partial vacuum inside the chamber. Steel bars line the windows to prevent deflection inward due to the pressure differential from the vacuum within. The galvanometer will be mounted above the

bed plate on steel bars. An opening was left for the implementation of a latching and sealing door. Inside the welded angle iron frame are four vertical T-shaped steel beams. These beams will be welded into the corners of the chamber to create a slot. These slots are intended to be lined with rubber strips and the viewing windows will be press-fitted into them. This will guarantee an air-tight seal, however, once the top of the box is welded together, these windows will be permanently fixed in place.

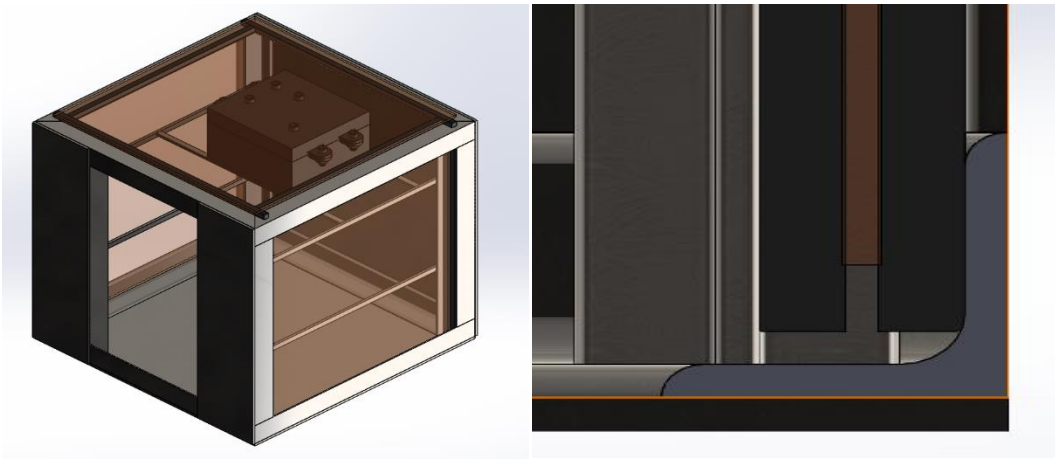

Figure 20: Angle iron chamber design with

The next design iteration of the chamber consisted of angle iron welded together with the viewing windows positioned on the outside of the frame. This design changed now allowed for a chamber that can be fully customizable. Each side of the box excluding the back-steel plate and the bottom of the chamber can now be fully removed. This allows experiments to be conducted in the chamber using camera equipment that may not be able to fit inside. However, placing the windows on the outside of the chamber makes it hard to structurally support them under a vacuum situation. To overcome this obstacle, the system would have to extract air from one port at the top of the chamber, while denser argon gas fills the chamber from a port at the bottom. This way the chamber will slowly fill up with argon as air is extracted and a vacuum will not be created. An airtight seal is still critical to maintaining a stable environment during the printing process. To account for this, the windows will be screwed into weld nuts that will line the outside of the box. Between the frame and the windows, a .5-inch-thick rubber strip will create a seal once the window is secured in place. The model of this design can be seen in Fig. 21.

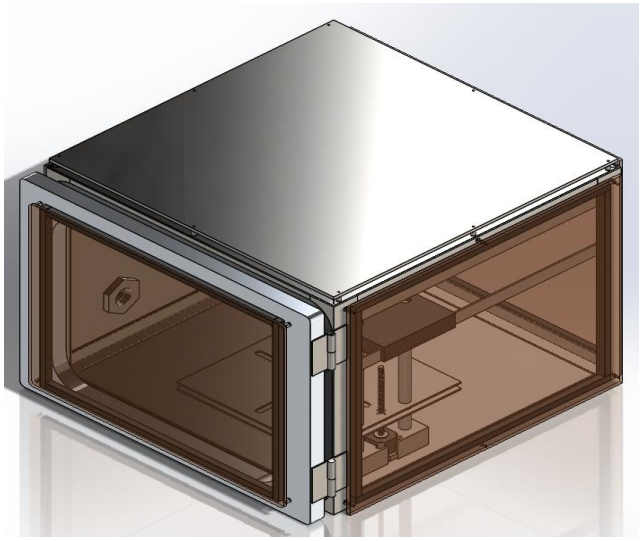

Figure 21: Angle iron chamber design with windows secured on the outside

To decide upon which design best fit our goals, a design matrix was used and can be seen below in Table 6. Each factor in the design was weighted by importance to this project. The four design options were: (1) rectangular tube steel with windows on the inside, (2) rectangular tube steel with windows on the outside, (3) angle iron with windows on the inside, and (4) angle iron with windows on the inside. The design matrix shows a clear choice that the angle iron frame with windows bolted to the outside would be the best for our project goals.

Table 6: Design matrix for chamber design

Design Criteria	Weight	Rectangular, Windows Inside		Rectangular, Windows Outside		Angle Iron, Windows inside		Angle Iron, Windows outside	
		Rating	Weight Score	Rating	Weight Score	Rating	Weight Score	Rating	Weight Score
Ease of Build	20	2	0.4	3	0.6	2	0.4	3	0.6
Efficiency	20	4	0.8	3	0.6	4	0.8	3	0.6
Cost	20	3	0.6	3	0.6	2	0.4	4	0.8
Customizability	30	2	0.6	4	1.2	2	0.6	5	1.5
Aesthetics	5	5	0.25	2	0.1	4	0.2	2	0.1
Safety	5	3	0.15	4	0.2	3	0.15	4	0.2
Overall Scores		2.8		3.3		2.55		3.8	

After choosing the overall design, the chamber then went through more iterations to meet all functional requirements. The initial size of the entire system was proposed to be 1ft. x 1ft. x 1ft. After analyzing the model, it was decided that there was not enough empty space inside the chamber. Since this system will be used for experimental purposes, empty space would allow for additions in the future, including a powder spreader, cameras, sensors, and experimental gas flow piping. Additionally, the galvanometer needs to be spaced at least 7 inches off the bed plate for the laser spot size to be accurate. The galvanometer would not be able to fit inside the box at this desired height. The box was then expanded to 2 ft. x 2 ft. x 1.5ft. The bed plate will now have about 10 inches of room between it and the argon inlet, which allows for custom piping and experimental set ups. Also, 2 ft^2 of empty area is behind the bed plate. This provides ample room for the addition of a roller and powder spreader in the future.

The back of the chamber will consist of a 1/8-inch-thick plate of steel that will be welded onto the frame. Two gas ports will be drilled into the plates to allow for inflow of argon and outflow of air. These ports were placed in positions so that the argon will flow over the bed plate and slowly fill the chamber from the bottom up while air exits at a port higher up on the chamber. The black steel nipple that will connect piping on the outside and inside of the chamber will be welded and sealed around the hole. A third hole will be drilled and filled with rubber or PVC piping to direct the USB cable out of the chamber, so it is accessible to the user. The backplate design can be seen below in Fig. 22.

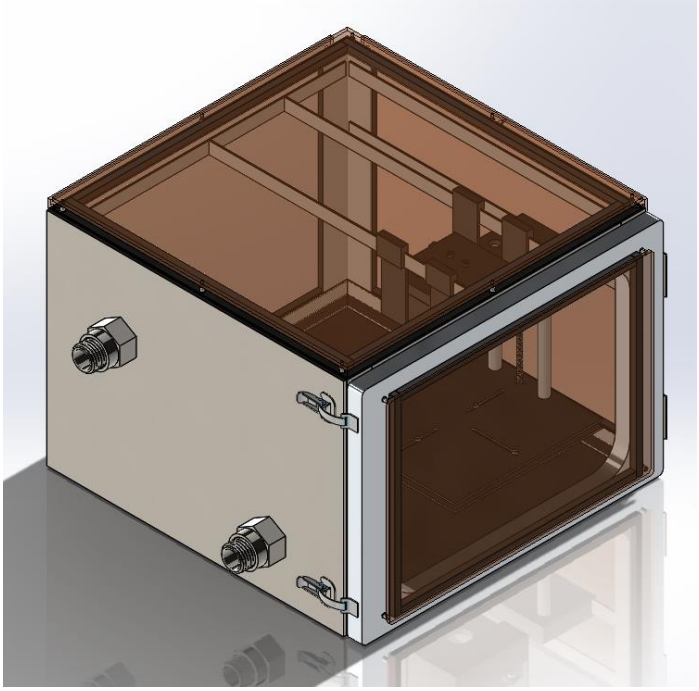

Figure 22: Air inlet and outlet ports

The galvanometer housing will be secured above the center of the bed plate inside the chamber. Steel bars will run the length and width of the inside of the chamber. From these steel bars the galvanometer will hang at the correct height. 3D printed hangers will hold the galvanometer in place but will also be adjustable for experimentation purposes. Since the galvanometer may need maintenance over time, it can be easily removed from the chamber by just lifting it off the hangers. An additional 3D printed support will mount below the galvanometer on a steel bar. This mount will hold the top of the bed leveling system in place, avoiding any unwanted movement. The CAD model of these 3D printed hangers and supports can be seen in Fig. 23.

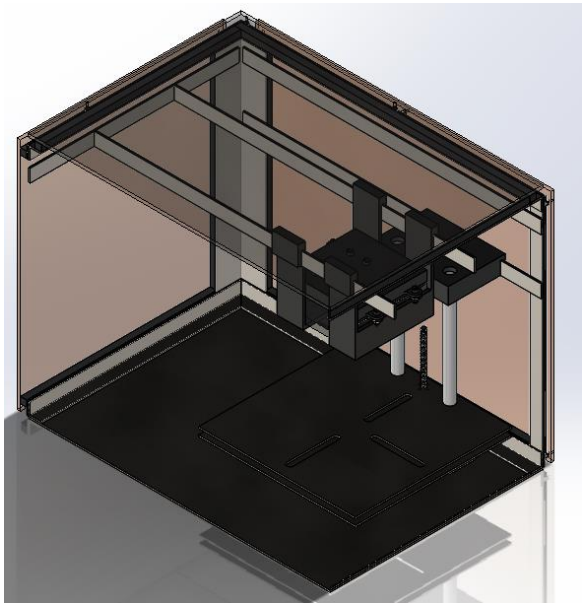

Figure 23: 3D printed Galvanometer and bed leveling supports

3.5.1 Window Sealing Rubber

The windows need to have a sealing layer between them and the frame of the chamber. A rubber sealing square will be adhered to the angle iron frame along the borders of where the windows will be placed. A #10 weld nut will be welded to the frame along corners and edges of the frame. The windows will be laser cut to match where these nuts are. With a ½ inch thick piece of soft rubber lining the frame, the windows will compress the rubber to 3/8 inches. This will create the seal needed to maintain an airtight chamber. Rubber comes in many different hardness factors, and it was critical to find the right type of rubber for this project.

To assess the kinds of materials that could be used for the compressive lining on the sides and door of the chamber, a Pugh matrix was completed with varying rubber compounds and can be seen below in Table 7.

Table 7: Pugh Matrix for determining rubber seal material

		Alternatives						
		1	2	3	4	5		
Criteria		Fabric-reinforced abrasion-resistant SBR	Abrasion resistant Polyeurthane	Economical SBR	Super cushioning abrasion resistant polyeuthane	High strength high temp silicone rubber	Totals	Rank
Machinability	0	0	0	0	+	+	2	1
Cost	0	0	0	+	–	0	0	7
Wear Resistant	0	0	–	–	+	0	-1	9
Compression	0	0	0	–	+	+	1	4
Dark color	0	0	0	0	0	–	-1	8
Durometer Hardness	0	0	0	+	+	0	2	1
Heat resistance	0	0	0	0	0	+	1	3
	0	0					0	
	0	0					0	
	Totals		-1	0	3	2		
	Rank		4	3	1	2		

It was determined that the “super cushioning abrasion resistant polyurethane” was the most suitable candidate for creating a compressive seal around the door. The durometer hardness is 50OO (50 durometers with the material being measured on the OO scale) which is subjectively soft and suitable for the application. The rubber is also highly compressive and elastic, meaning it will compress and then return to its original state after compression.

3.5.2 Design of Chamber Peg Stands

To ensure the working environment of the LPBF system is always level, and that the build plate is normal to the ground, a leveling system must be installed into the chamber itself. The surface that the LPBF system is placed on may not always be perfectly level, which means that the leveling system must be capable of incremental adjustments. This was addressed in the chamber design mechanically, by adding 3/8-16 flanged rounded weld nuts onto each corner of the chamber base. Through holes were to be cut under each weld nut to allow for a 3/8-16 high-strength hex screw to be fixed in place and extrude out through the bottom of the chamber where the head is rested into cavities in 3D printed peg stands, and bonded with a metal-polymer compatible adhesive (Fig. 24).

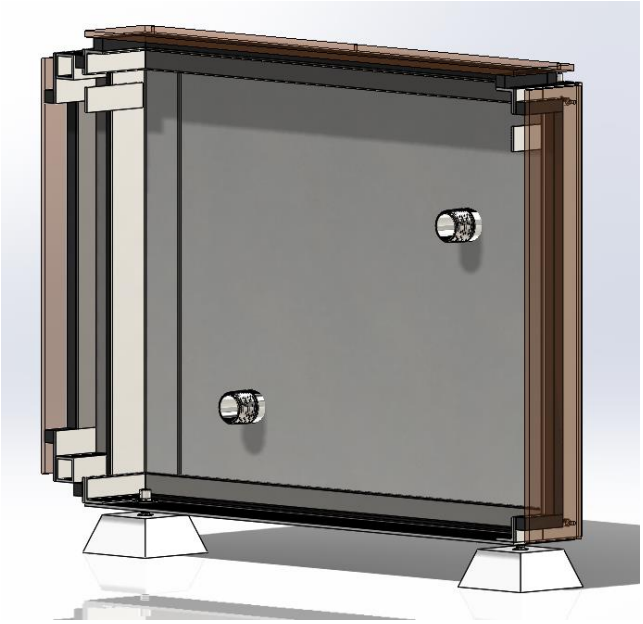

Figure 24: Peg stand design

To ensure that the hex screws and threaded weld nuts can withstand the stress of the chamber, and to ensure that the screw-nut interface would be self-locking, static force calculations were done. A notable assumption while calculating the stress in the screws is that each screw is subject to the same load. Realistically, the load on each screw would differ slightly based on its planar distance from the chamber’s center of gravity. However, to ensure each screw can withstand the load of the chamber to a liberal degree of safety, it was assumed that each screw would take on half of the load of the chamber. Fig. 25 shows the free body diagram for the forces acting on the hex screw in a state of static equilibrium. Table 8 below provides variable definitions for the diagram.

Table 8: Forces on Peg Stand

Variable	Definition
W	Axial Load (Chamber weight / 2)
Wr	Axial Load Reaction Force
N	Normal Force
F_f	Frictional force = μ*N
P	Pitch Length = Lead Length
Alpha	Lead Angle

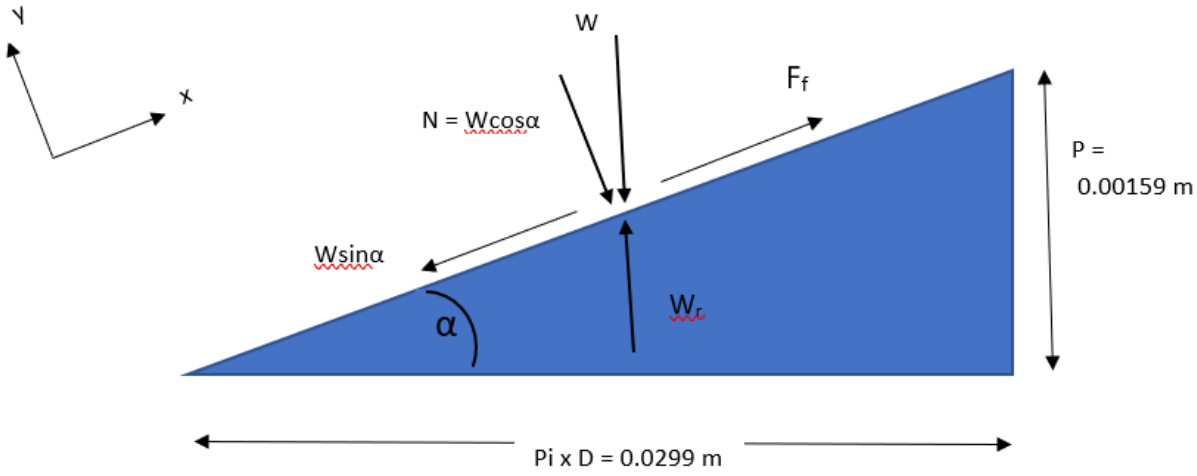

Figure 25: Peg stand thread Free Body Diagram

Calculations

The ultimate tensile strength of the hex screw is approximately 1.034 GPa based on its data specification sheet. This means that the stress applied to the screw cannot exceed this value without failure. The stress applied to the screw is equivalent to the axial load divided by the effective area of the thread that is incurring the load. The calculations are as follows:

Axial Load "W" = Total weight of chamber / 2 = 663.65 N / 2 = 331.825 N

Tensile stress area of 3/8-16 UNC thread = 0.077 in^2 = 0.0000497 m^2

Tensile stress acting on thread = 331.825 N / 0.0000497 = 6.68 MPa

6.68 MPa << 1.034 GPa

The screw will not fail under this loading condition.

The screw/nut assembly must be self-locking to ensure that no movement would occur when an axial load is applied from the weight of the chamber. The definition is more clearly explained by emweb.unl.edu: "A screw is considered self-locking if the lead angle is selected such that in the absence of a screwing moment (i.e., M=0) the force will remain less than $\mu_s N$ so that the threads

will not slip relative to each other. The maximum thread angle for the screw to be self-locking is given by setting $\mu_s N$

The calculations for this loading condition are as follows:

Axial Load "W" = Total weight of chamber / 2 = 663.65 N / 2 = 331.825 N

Lead angle for single-start thread = Arctan (Pitch length / Thread Circumference)

= Arctan (0.00159/0.0299) = 3.04º = Alpha

Wcos α = Normal Force = 331.35 N

Force of friction = μ*Normal Force

Coefficient of friction for zinc-coated steel on zinc-coated steel "μ" = 0.6

0.6*331.35 N = 198.81 N

Wsin α = Force opposing friction = 17.60 N

17.60 N << 198.81 N

The screw-nut assembly is self-locking.

3.6 Bed-Leveling System Design

3.6.1 Design Iterations

Pictured in Fig. 26, the initial concept design of the printing bed system was created using the simplest mechanical systems possible. This concept featured a four-post lifting and lowering system that would manually be controlled by the operator of the printer. This model was created with structural toughness being the key feature. The overall usable printing area is 10" x 10". The size of the plate is slightly bigger; however, the size of the powder roller is restricted by two of the posts. While this design is tough and reliable, it did not meet the constraints that were given to us.

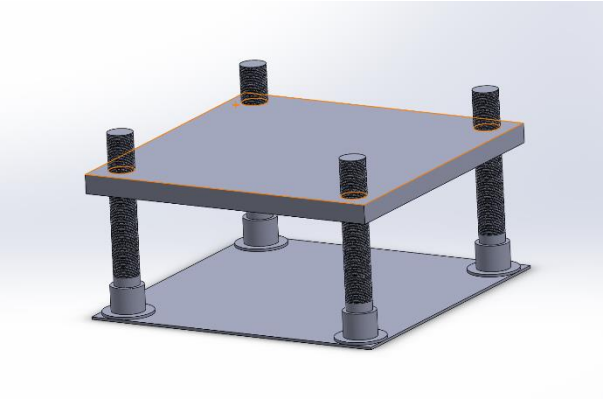

Figure 26: Initial bed leveling design

The second design, shown in Fig. 27, was a complete redesign of the printing bed system. This design had several added features to accommodate the constraints the system must fulfill. This included an adjustable plate which could fixture a removable printing plate on top, which means multiple printing plates could be made depending on what material is being used. Two brackets are in preset holes that secure the new plate in place. The holes in the plate can accommodate printing plates from 12” x 12” down to 2” x 2” squares. The second improvement on the design would be the two-post support instead of the original four post. After careful calculations, the conclusion was drawn that four posts were not needed to provide stability, thus created more working space inside the printing chamber. The next major upgrade was installing a motor on a centralized shaft that would raise and lower the bed automatically. The stepper motor chosen yields an 18-micron elevation change per turn, which fulfills the requirements. Lastly a steel plate was added on the bottom to house the motor and support beams in one closed loop system. Now the bed can be completely removed and modified or replaced and installed back into the printing chamber.

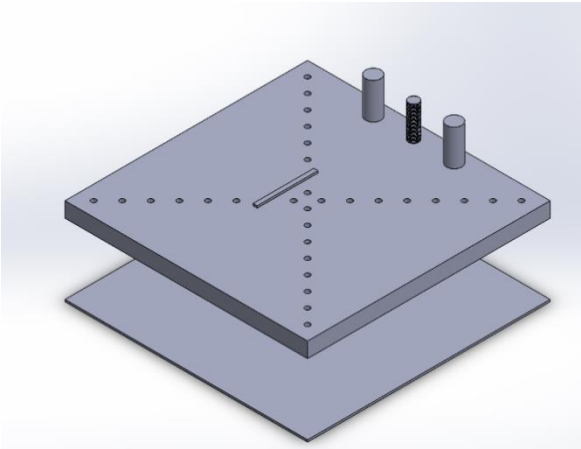

Figure 27: Bed leveling design with dowel pin holes

After further research and concept testing, a third design of the printing bed was created and can be seen in Fig. 28. This design aimed to increase the efficiency and lower the cost of manufacturing the bed. Sliding bracket fixtures that consist of a socket head screw and a nut were designed to accommodate a wider selection of printing bed materials that could potentially be in a non-square shape. The sliders will be moved into position and then tightened down on the bottom of the plate housing. The sliders will only fixture the working piece on three sides as to allow a future powder spreader to not run into any obstructions. The motor incorporates a threaded shaft that will turn to lower and raise the bed. Additionally, to keep this prototype customizable, the bed plate will be secured to the bottom of the chamber with a machined base. This base will add structural integrity to the bed leveling system and will also allow for the bed leveling system to be removable for repairs. The final iteration of the printing bed exceeds the design requirements, while remaining easy to use.

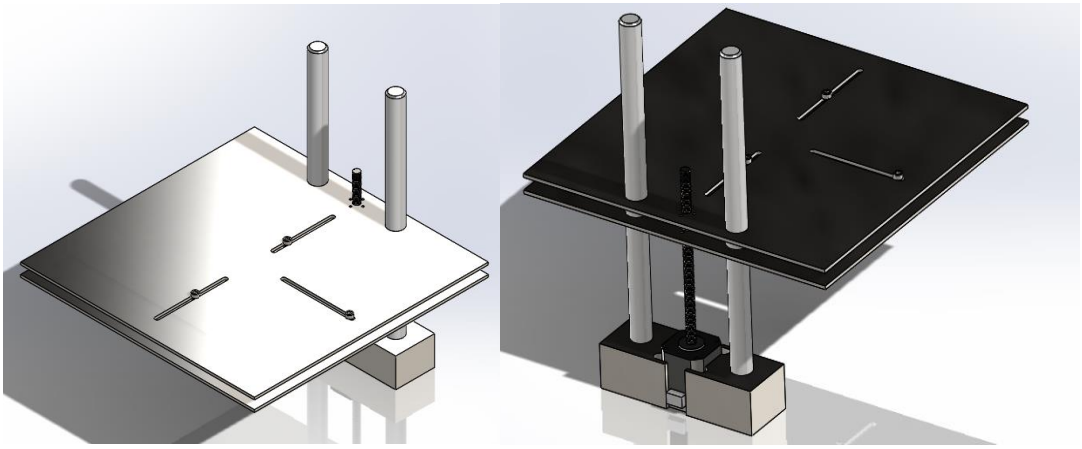

Figure 28: Final bed leveling design

A design matrix was created to weight the design options and can be seen in Table 9. It was clear that the final design would be superior in functional requirements, as well as many other categorizes listed below.

Table 9: Design Matrix for bed leveling system

Design Criteria	Weight	Initial Design		Dowel pin design		Sliding bracket design	
		Rating	Weight Score	Rating	Weight Score	Rating	Weight Score
Ease of Build	20	5	1	2	0.4	3	0.6
Efficiency	20	1	0.2	1	0.2	4	0.8
Cost	20	4	0.8	3	0.6	4	0.8
Customizability	30	1	0.3	4	1.2	5	1.5
Aesthetics	5	3	0.15	2	0.1	3	0.15
Safety	5	2	0.1	4	0.2	4	0.2
Overall Scores		2.55		2.7		4.05	

To future improve upon this design, a few changes were made. A 3D printed motor cap was created to fit tightly around the machine base. This motor cap will ensure that the motor remains fixed in place while it moves relatively heavy loads up and down. The motor cap will be screwed into place on the sides of the machined base. Next, to cut down on weight of the system, and to improve stability, the two-plate design was reconsidered. Using just one bed plate would cut down on weight and money and still allow for the use of the slotted fixture design. It is essential that the bed plate always remains parallel to the galvanometer system. This requires that the bed plate be securely fastened to the vertical shafts on which it will slide. To account for this, lightweight aluminum linear shaft bearings will be implemented onto the shafts and sit inside of the bed plate. To fixture the bed plate to the linear shaft bearings, bearing housings will be implemented into the design. In order to secure the housings to the bed plate in a permanent way, welding was considered. Since TIG welding is required for aluminum welding, an alternative method must be considered since our project group does not have experience in TIG welding.

Using JB-Weld epoxy, the bearing housings will be permanently secured to the bed plate. The final bed plate design with these added features can be seen below in Fig. 29.

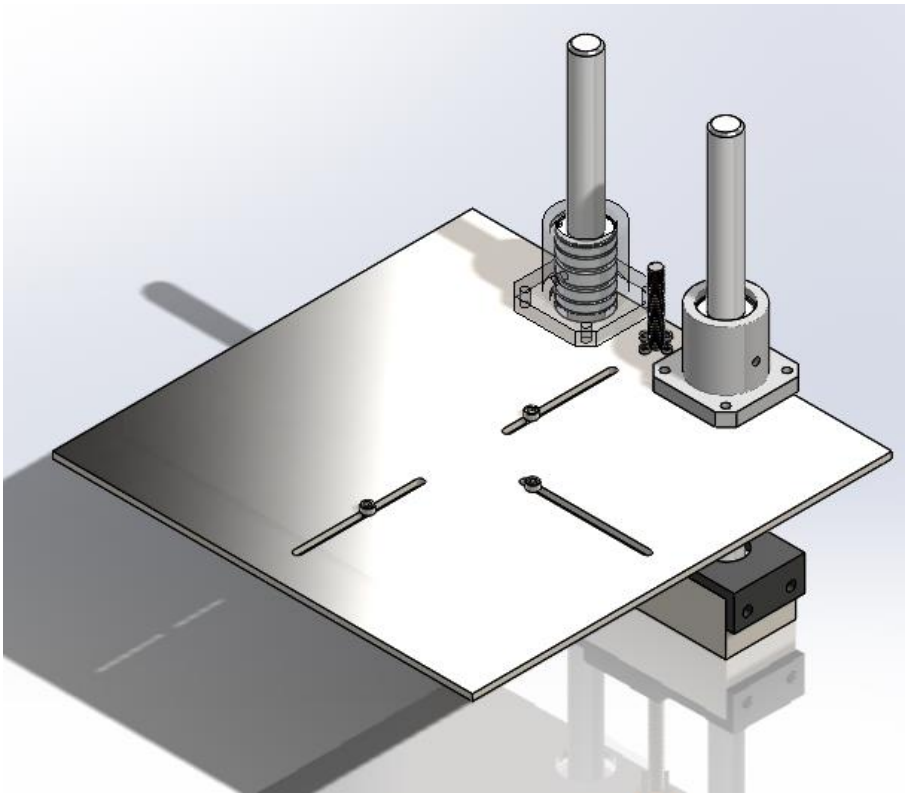

Figure 29: Final bed leveling system design

3.6.2 Material Selection

The materials that were selected, according to Table 10, were chosen for their high strength and proven reliability over constant loading and unloading stresses. The overall weight over the printing bed system, including all subcomponents, is 14.5 lbs. The bed plates were chosen based on resources available to cut a desired design into them. Since a water-jet cutter will be the means of manufacturing the bed plate, aluminum was the best choice. Additionally, aluminum is significantly lighter than steel which will cut down on any moment forces acting on the lead screw from the motor.

Table 10: Material list for bed leveling system

Subcomponent	**Material Selection**
Printing Bed Plate	5052-H32 Aluminum Plate
Screw Jack	High Strength Steel
Rear Support Columns	Chrome Plated 1045 Steel
Machined Base	Low Carbon Steel

3.6.3 Free Body Diagram and Torque Calculations

The calculations for the bed system were highly important to understand how much force is being put on each component in the system. This cantilever design was a concern at first because a moment could impact the way the lead screw performs. This was mitigated by attaching a 3D printed support on the top of the vertical shafts that will be fixtured to the frame of the box. This cancels out all moment forces on the sides farthest from the motor, resulting in the lead screw only having to lift the forces from the weight of what is on top of it. To ensure the motor selected will have enough torque to raise the weight of the bed plate, as well as any substrate on top of it, torque calculations were derived from free body diagrams shown in Fig 31. The total torque needed was found and then a motor was selected.

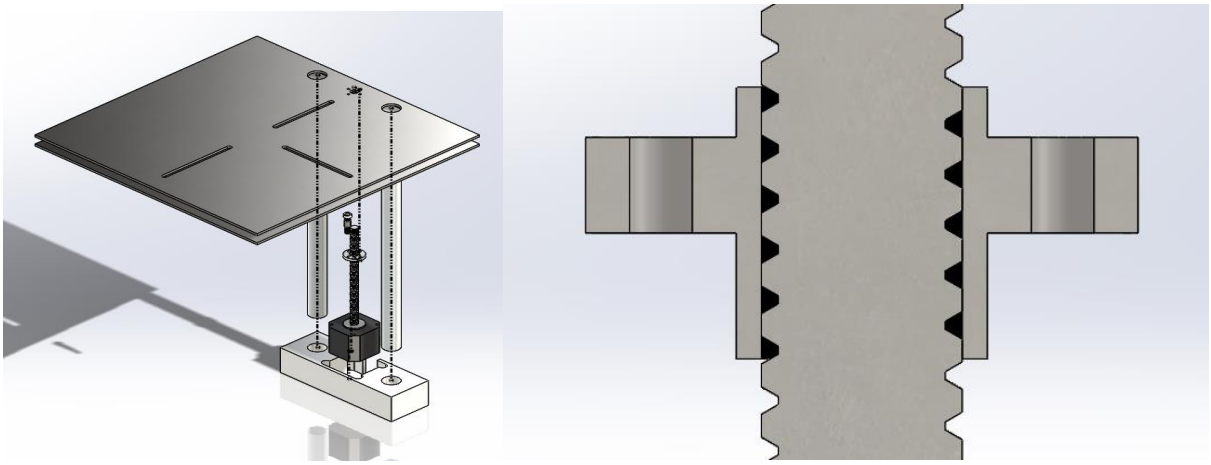

Figure 30: Section view of threaded Z axis motor shaft

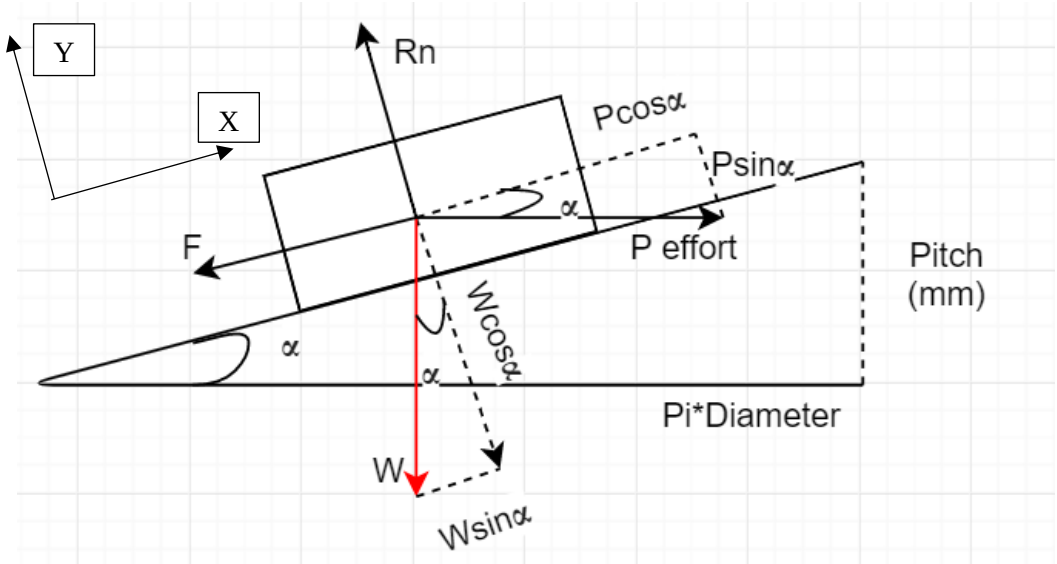

Figure 31: Motor threaded arm free body diagram

Table 11 denotes what each variable represents in the free body diagram of the square threaded screw portrayed above.

Table 11: Forces on bed leveling system

Variable	Definition
F	Frictional force = μ*R_n
Rn	Normal Force
P	Effort to move lead screw
W	Load on thread
Alpha	Thread Angle

Calculations

The first step in finding the torque on the motor is finding the thread angle of the selected thread. For this lead screw, a TR8x8 thread will be used. This is a square threaded lead screw, hence the square depicted in the free body diagram. The diameter of the screw is 8mm and the pitch is 8mm as this thread has 4 thread starts, spaced 2mm apart. This means per revolution; the nut will move 8 mm due to the 4 thread starts.

$$tan \propto = \frac{Pitch}{\pi * d}$$

$$\tan^{-1}\frac{8mm}{\pi * 8mm} = 17.66\ degrees = \propto$$

An equation for torque must be derived based on the equilibrium condition of the lead screw.

*Force in * direction*

$$\sum F_x = 0$$

$$Pcos \propto\ -\mu R_n - Wsin \propto = 0$$

Therefore:

$$Pcos \propto = \mu R_n + Wsin \propto \qquad \text{(eq. 1)}$$

Forces in Y direction (perpendicular to the plane)

$$\sum F_y = 0$$

$$R_n - Wcos \propto -Psin \propto = 0$$

Therefore:

$$R_n = Wcos \propto +Psin \propto \qquad \text{(eq. 2)}$$

Combining R_n from eq 2 into eq 1 results in:

$$Pcos \propto = \mu * Wcos \propto +\mu * Psin \propto +Wsin \propto$$

Separating the load forces and the effort to move force results in

$$P(cos \propto - \mu sin \propto) = W(sin \propto + \mu cos \propto)$$

$$P = W \frac{sin\propto + \mu cos\propto}{cos\propto - \mu sin\propto} \quad \text{(eq 3)}$$

From equation 3, actual effort applied to raise the bed leveling load can be calculated

Since torque = P * r, multiplying equation 3 by the radius of the thread, torque can be calculated

Assuming a 5 lbs substrate being placed upon the 14.5 lbs bed leveling system, a total of 20 lbs can be used as the load on the lead screw. Therefore W=20 lbs or 88.9644 N.

Assuming the lead screw has machine oil on it to reduce friction, the coefficient of friction for a lead screw on a steel to steel contact surface would be 0.15.

$$P = 88.9644 \frac{sin17.66 + .15 * cos17.66}{cos17.66 - .15 * sin17.66} = 43.76\ N$$

Torque = 20.67 N * 4mm = 175 N*mm

As most motor torques are listed in N-cm or oz.in, the following conversions were used

$$175N * mm * \left(\frac{1cm}{10mm}\right) = 17.5\ N - cm$$

3.6.4 Bed-Level Motor Selection

Based on the motor torque calculated above, a motor was selected to exceed this torque requirement in the case of heavier loads applied to the system. This will give the system a safety factor to avoid unwanted wear and tear on the system. When choosing motor, a small incremental step sizes to the micrometer were needed for the LPBF system to operate as intended. Additionally, to avoid any unwanted movement within the system, a motor with an integrated lead screw was desirable as this would eliminate the need for shaft couplers to secure the lead screw to the motor arm. The motor selected for use is the Redrex Nema 17 Stepper motor which will run at 1.5A and have torque capacity rated at 40Ncm. This Nema 17 motor has 200 steps per revolution which results in .04 mm per step or 40 microns. This exceeds the torque required in the system, satisfies the step increment requirements, and meets within the budget of this project. A picture of the motor can be seen below in Fig. 32.

Figure 32: Nema 17 Z axis stepper motor

3.6.5 Electrical Wiring of Bed Leveling Stepper Motor

For the bed leveling system to operate correctly, a few necessary electrical components will be discussed and can be seen in Table 12. To give an overview of how the bed leveling system will operate, a Nema 17 stepper motor will first position itself with respect to the galvanometer. Since stepper motors do not know their spatial positioning, a toggle switch will be positioned on the base of the LPBF printer below the bed plate. The stepper motor will activate, and lower down until it reaches the toggle switch. Once the toggle switch is activated, the bed leveling system will then move a set distance up, so that it is exactly 181mm from the output port of the galvanometer. This is the working distance for the F-theta lens that will be retrofitted into the design once it is purchased. Next, the bed plate will be designed to lower a step (40 microns) after each layer is complete. To ensure this is a seamless process for the user, the following electrical components are used (table 12) and positioned as pictured below in Fig. 33.

Table 12: Electrical component list for bed leveling system

Component	**Use**
Solderless Breadboard	Electrical set up and positioning
Nema 17 Stepper Motor	Motor for bed leveling system
Toggle Switch	For bed positioning
A4988 Motor Driver	Driver for input power and logic power to move motor in desired motion
Arduino Uno Microcontroller	Microcontroller to input code from PC
12V 1.5 Amp 2.1mm jack Wall adapter	12V power supply for motor

Female Jack Adapter Term BL to 2.1mm Plug	To provide one power rail of the breadboard with 12V of power

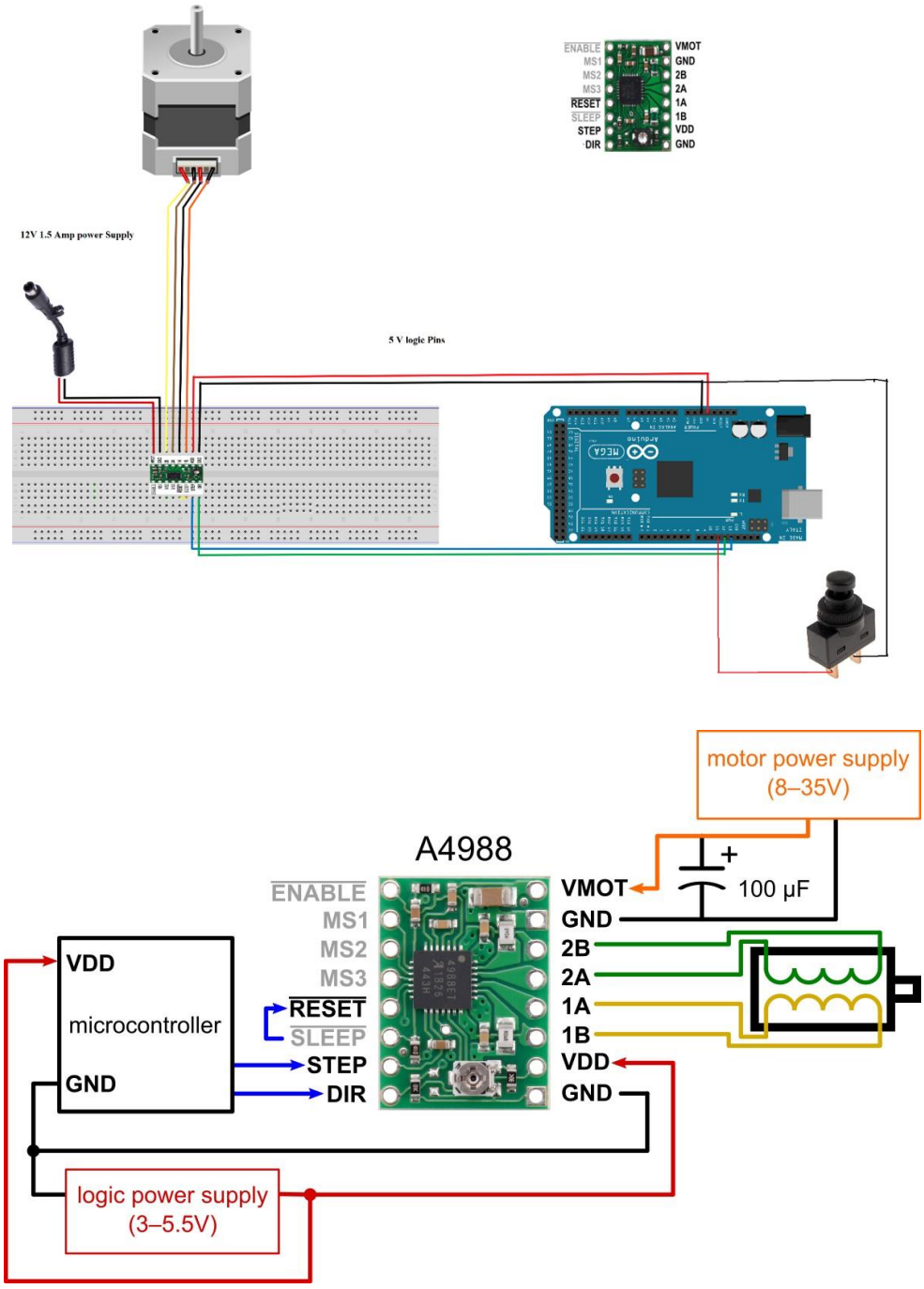

Figure 33: Wiring schematic for bed leveling system

To ensure the motor is receiving the correct amperage, the user may have to turn the potentiometer on the A4988 driver until the motor is receiving 1.5 A. The motor will not run properly if this is not calibrated correctly. Some addition points to note are that the sleep and reset pins on the A4988 driver must be wired together or else the motor will not run. Additionally, a 100 micro farad capacitor wired between the voltage and ground for the motor power supply is optional but will protect the motor from voltage spikes that may occur during operation. Since this motor function is relatively basic, high spiking voltage is unlikely to occur. After this wiring set up is complete, the Arduino nano used on the galvanometer was replaced with this Arduino Uno. This means that both the galvanometer and the bed leveling system will run on one microcontroller and under one code.

3.7 Door Design

When considering the design for the door system, it was important to revisit the considerations identified previously. The door must be capable of creating a firm seal to maintain an airtight internal area. The door must also have a viewing window installed on the front. Lastly, the door must be removable for convenient access to the chamber's internal components and build platform. Initial ideation for the design involved a brainstorm session where further necessary details were identified. To create an airtight seal, the door must feature a highly compressive lining that presses against the exterior wall of the chamber. Further research of airtight chamber doors allowed for development of a prominent design concept.

The initial design for the door consists of a metal block fixtured to the side of the chamber frame via door hinges and latching locks. A ½ inch wide slot will run the perimeter of the inside of the door to house the rubber lining which will create a seal with the chamber upon closing. This slot will help maintain the rubbers seal after repeated usage. A rubber lining will run along the perimeter of the viewing window. Fig. 34 shows the CAD model for this design.

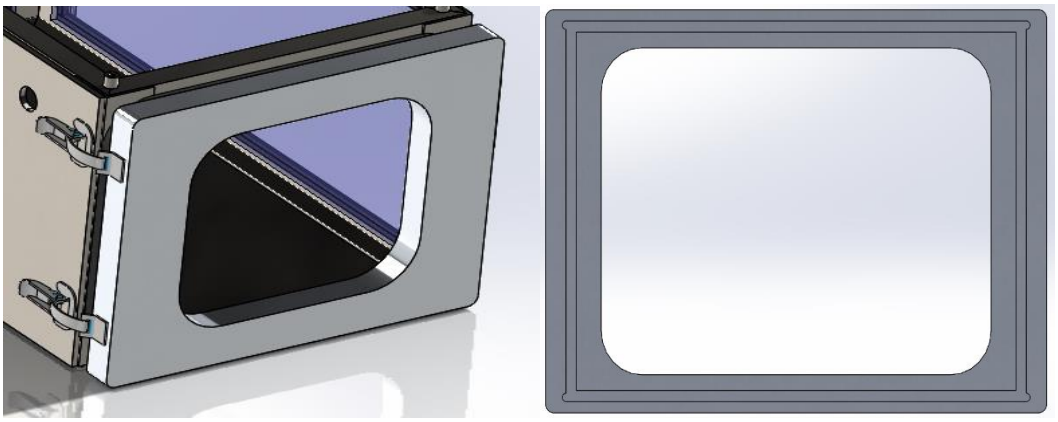

Figure 34: Initial door design

The door hinges and draw latches are to be welded to the exterior of the chamber frame, which means they cannot contain hazardous elements such as zinc that could create toxic fumes when exposed to extremely high heat. The selected material for the hinges and latches is to be steel. The door hinges selected must be lift-off hinges to allow for the easy removal of the door for

any future adaptations to the chamber or maintenance. For determining the kind of metal that the door should be made of, a Pugh matrix was created with different material candidates selected as the "concepts". Table 13 shows the Pugh matrix for the door. It was determined that Aluminum was the ideal candidate based on the ranking outcome of the matrix. Aluminum is a desirable material because of its machinability, low weight, and resistant to wear and corrosion when compared to the other material candidates. While it will cost more than steel, the light-weight aspect is a necessary property due to the large size of the door. The machining of the door was outsourced to manufacturing company because of the impracticality of machining it in the manufacturing labs on campus at WPI. The stock piece of aluminum was simply too large to fixture in any of the CNC machines available on campus. To compensate for this, detailed technical drawings and CAD models for the door design were sent to the manufacturing company.

Table 13: Pugh Matrix for determining door material

		Alternatives						
Criteria	Baseline	Stainless Steel	Low-Carbon Steel	Iron	Aluminum		Totals	Rank
Machinability	0	0	0	–	+		0	6
Cost	0	0	0	0	–		-1	8
Weight	0	0	0	–	+		0	6
Abrasion Resistance	0	0	–	–	+		-1	9
	0						0	
	0						0	
	0						0	
	0						0	
	0						0	
	Totals		-1	-3	2			
	Rank		2	3	1			

The machine shop used to fabricate the door could not guarantee they had the time and resources to make our part. Therefore, a second door design was considered that would be easily manufacturable on campus. The second door design would consist of steel tubing and bars that could be welded together into a door. This design aimed to lower budgeting costs while meeting the same demands of the previous door design. Although the desirable material Aluminum could not be used for this door design due to weldability issues, the door would now be hollow which would keep the weight relatively light. Additionally, now that slots could not be engraved into the inside of the door for the rubber lining, it was decided that the rubber lining would be secured to the chamber instead of the door. Models of the second door design and the finished CAD model of the LPBF system can be seen in Fig. 35 and Fig. 36.

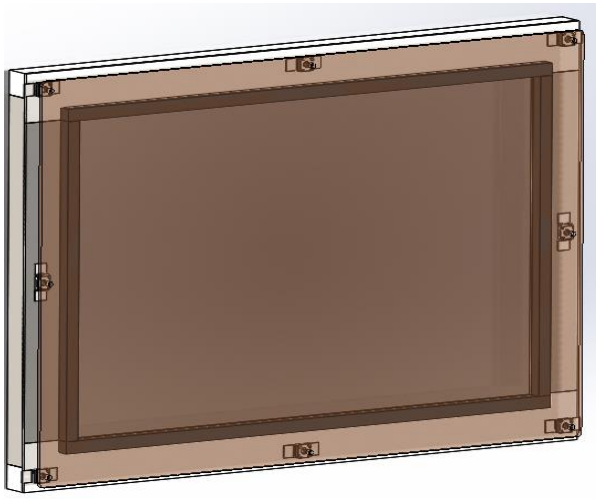

Figure 35: Final door design

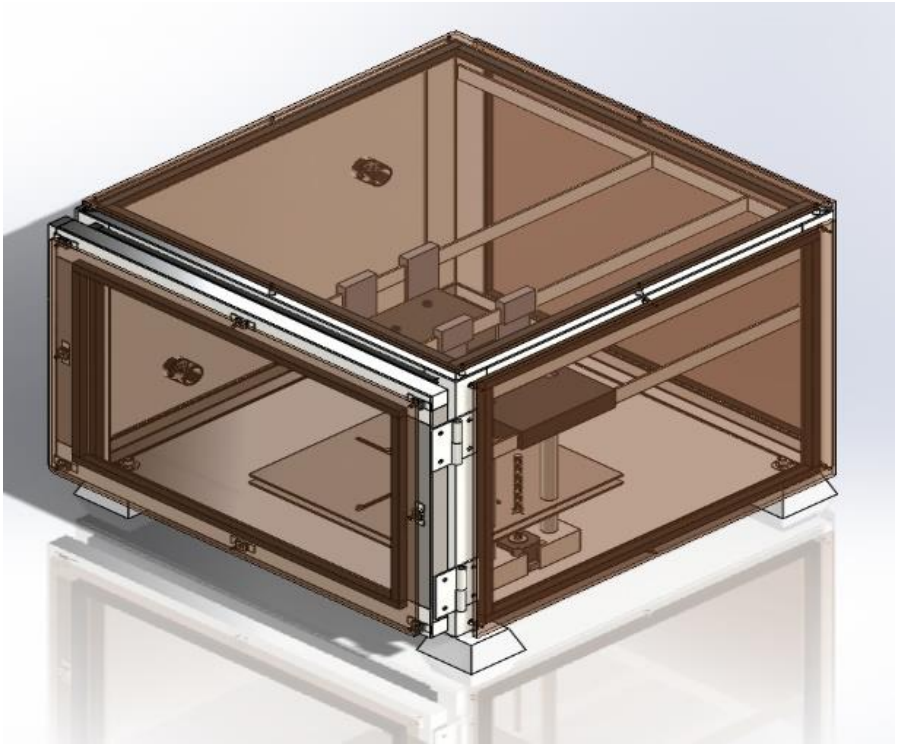

Figure 36: Final LPBF system design

4.0 Fabrication

Fabrication of the PBF system and its relevant components was confined to utilizing the various manufacturing resources available on WPI's campus. Housings and other non-loaded components were 3D printed in ABS in the Foisie Innovation Studio Prototyping Lab. Most components were

machined, welded, and hand-tooled in the Washburn Shops on campus. This included structural components such as angle iron and steel plating, the acrylic windows and the compressive rubber lining for sealing of the windows. Specific parts for component interfacing and establishing electrical connections were ordered from various hardware suppliers and fixtured to the LPBF system via methods described above. A breakdown of the fabrication process for the individual sub-assemblies is described below.

4.1 Chamber Fabrication

When planning to manufacture the frame of the LPBF prototype, the strength and weldability of the structure was the most important parameters that needed to be met. Steel angle iron at 2” x 2” x .125” was ultimately chosen to construct the outside of the frame. Steel was chosen over other metals such as aluminum because of its weldability. Since the project group had minimal welding experience prior to this project, MIG welding was the preferred type of welding for non-experienced welders. With a steel frame, various other components constructed out of plain steel could be easily fastened to the frame through MIG welding.

Upon constructing the box frame of the chamber, various iterations of the chamber at a smaller scale were fabricated to practice techniques to make the final version as structurally sound as possible. The main issue faced during the fabrication of the chamber frame was the cuts used to mate the angle iron together in a box shape. In the first attempt, miter cuts, or 45-degree cuts were made on the angle iron. Due to human error and possible calibration errors in the table saw protractor, the angles never perfectly aligned to create a seal and a square corner. To fix this problem, cope joints were used on the angle iron. Cope joints involve cutting out a part of one of the angle iron members so that the joining member will fit in place like a puzzle piece. This resulted in less cutting needed, and less human error involved as cuts needed to be straight and not angled. A cope joint cut that is prepared to be MIG welded together can be seen below in Fig. 37.

Figure 37: Square cut of angle iron frame

Due to the low cost of the steel being used, three chamber iterations were created to perfect the skill to create a square and sealed chamber frame. While creating the iterations, the size of the final prototype was decided upon based on available space that would be inside the chamber to allow for additions to be made within in the future. A picture of the various size chambers produced can be seen below (Fig. 38).

Figure 38: Welded chamber frames

Once the frame was complete, the steel rail system consisting of 1” x .125” steel rectangular bars that will support the galvanometer and the bed plate were welded into their respective positions. The rails that span the length (door side to back side) of the chamber spaced 6 inches apart will hold the galvanometer in place. An additional rail runs along the windowed side of the box above 4 inches from the top angle iron. This rail will support the top of the bed leveling system by eliminating any moment forces on the steel support shafts with a 3D printed part.

After the rail system was welded into place, the windows on the side, back and top were prepped for completion. The acrylic windows were first laser cut to have screw clearance holes on the perimeter of the window area to allow a screw to hold it into place. Once the acrylic sheets were properly cut, screws were placed in the holes and fastened to weld nuts. With the windows and the weld nuts attached, the windows were positioned onto the chamber frame. Each weld nut was then carefully welded into place, ensuring the windows were centered over the chamber openings. After the welds cooled, the rubber lining was prepped for installation. The rubber came in a 3’ x 6” sheet and needed to be cut down into .5” wide sections at necessary lengths. A hot wire cutter, as well as a heated knife, were used in cutting the rubber down into sections. After the rubber was cut, a rubber to metal elastic Loctite glue was used to secure the rubber along the chamber frame. The windows were then reattached, and the glue was left to dry into place. The glue created a solid seal on the rubber and the windows pressed firmly onto the rubber seal allowing for no visible air gaps into the chamber. Upon completion of this step, the chamber now had removable viewing windows that can be easily replaced in the future with laser safe viewing window glass (Fig. 39).

The final step in the chamber fabrication was welding on the last remaining features of the prototype. First, the floor of the prototype consisted of a .125” thick sheet of steel and was welded onto the bottom of the frame. Next, a second panel of steel was first predrilled before welded onto the frame. These drill holes will be where the argon inflow and air exhaust will be located as well as a port for electrical wiring and a future fiber optic cable. The argon inflow hole is purposely positioned on plane and adjacent to the bed leveling system to allow for steady laminar flow of argon over the bed plate during operation. This is how commercial LPBF work and this set up will allow for experiment pipe arrangements to meet the flow demands over the bed plate in the future.

Once the side steel panel is welded into place, two gas flow nipples are welded into the predrilled holes.

Figure 39: Chamber with viewing windows

4.2 Galvanometer Fabrication

The galvanometer was fabricated to be cheap, yet functional within the chamber. Two galvanometer systems were created and tested to ensure this. Once the designs were solidified, the baseplate for the galvanometer system was 3D printed and the electrical components were placed in their respective positions on the baseplate (Fig. 40). The system was tested using a laser pointer to ensure the mirrors worked in deflecting a beam into a desired shape.

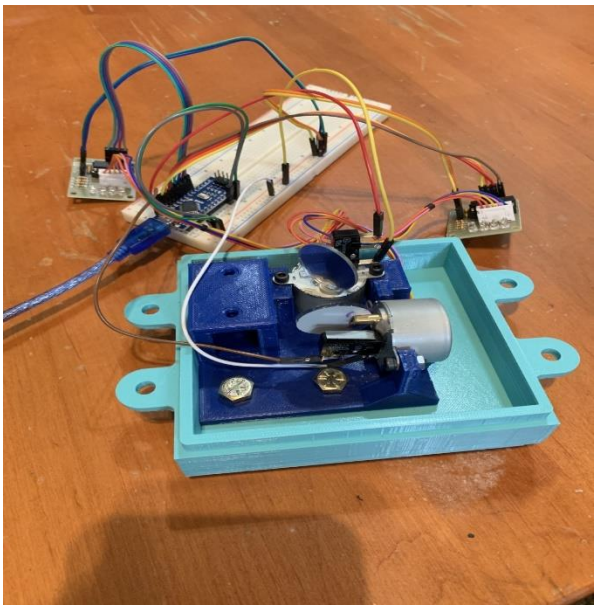

Figure 40: Galvanometer in 3D printed housing

Once this was complete, a new galvanometer with an improved design was 3D printed using ABS. This material will reduce the chances of the laser causing too much heat within the system and warping any of the plastic components. With the new galvanometer system printed, the baseplate was secured to the top of the housing and the f-theta lens port was secured on the bottom of the housing. The wiring was bundled and fed outside of the housing to the top, where the electrical components will be secured. The galvanometer was then hung inside the chamber from 3D printed hangers and tested. An image of the galvanometer testing within the chamber can be seen in Fig. 41.

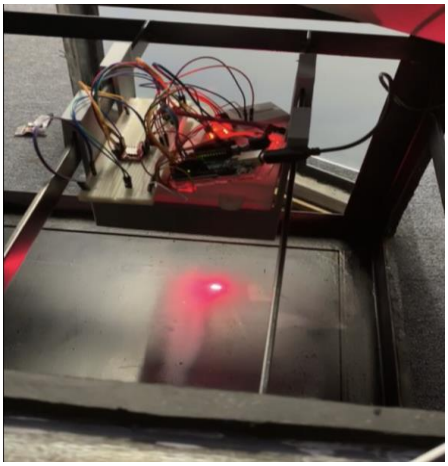

Figure 41: Galvanometer implemented into chamber

4.3 Bed-Leveling System Fabrication

The bed leveling system fabrication required careful design and tolerance considerations. This system must move relatively heavy loads (around 15 lbs.) at very small increments for many repetitions. The system must be built carefully and accurately to ensure smooth and repeatable movements. To start, a CNC machined based was created. A housing for the z-axis motor and two chrome plated steel support shafts were milled into a steel stock. The motor slot was milled with a clearance tolerance as it was important that motor sat flat on the bottom of the base without any obstructions. The ¾” steel support shafts were fitted into tightly tolerance (+.0005”) dowel pin holes. This completes the base of the bed leveling system.

Next, fabrication of the bed plate was done. A Wazer Desktop water jet cutter was used to punch out the design shown in Fig. 29. Due to the machine limitations, only one bed plate was able to be created to the intended design, so the bed leveling system design changed from two aluminum bed plates stacked on top of each other, to just one bed plate. With the 5052 H32 Aluminum bed plate cut out, linear motion shaft bearings were slotted onto the support shafts. The linear shaft bearings were then secured inside of bearing housings using a retaining ring. In order to make a permanent bond between the bearing housings and the bed plate, JB weld was used. Aluminum and steel cannot be MIG welded together which is why this epoxy solution was used. Once the JB weld is dried and secures the bearing housings to the bed plate, the bed leveling system fabrication is complete. The final step in the fabrication process involved welding the base to the floor of the chamber and attaching the 3D printed support to the top of the vertical shafts. A

finished picture of the bed leveling system cannot be produced due to unforeseen issues which will be discussed at the end of this report.

4.4 Door Fabrication

The design of the door had to be revisited during the fabrication phase of the project due to the inability to outsource the machining job. Initially, our team had decided to have a large piece of stock aluminum be machined by a third-party to create the shape of the door because the CNC machines available at WPI are too small to fixture a piece of metal the size we needed. However, communication challenges with this manufacturer required us to redesign the door to be fabricated in house using on-campus resources.

The new door design involved miter cutting and MIG welding members of square cross-sectional tube steel together to form the door frame. Miter cuts were necessary during this part of the fabrication due to the square cross section of the steel used. Any air gaps that resulted from human error during cutting of the steel members will be fixed with Flex Seal during testing. Next, steel bars 1.5” wide were welded over the door frame to add surface area to the exterior of the door. The rubber lining was then applied to the perimeter of the exterior of the door viewing port to create a seal with the viewing window that would be placed there. Weld nuts were welded into place using the same process as done in the chamber fabrication. A rubber lining was also applied to the outside of the chamber along where the door would come into contact with the chamber frame.

Once the door was manufactured and the rubber lining had dried, the door was then welded onto the chamber frame with hinges and door latches. The hinges were first welded onto the chamber frame in such an orientation that a user could lift the door upwards when it is open to remove the door completely from the assembly by using the lift-off hinges. The latches were then welded on to ensure the door firmly seals shut. Fig. 42 below shows a photo of the door frame assembled on the chamber body.

Figure 42: Chamber with door frame assembly

5.0 Results and Conclusions

Note on COVID-19 Pandemic

Due to the global pandemic surrounding COVID-19, fabrication of the LPBF system had to be suspended and ultimately cancelled. WPI promptly enforced quarantine procedures to ensure the safety and well-being of the faculty, staff and students. Essential resources related to the project such as manufacturing equipment and lab access were inaccessible at this time. The team utilized this project opportunity to understand and develop design and manufacturing procedures identified for development of this economical LPBF system. Results and conclusions for this project touch on the final status of the fabricated system with a focus on different components in the assembly, what steps could be taken to complete the assembly, and any future optimization/studies that could be done in conjunction with the completed system.

5.1 Final Status of LPBF System

All design procedures/documents were completed prior to fabrication. This includes the final iteration of the 3D assembly in SolidWorks, material selection charts and matrices, static stress analysis on the load-bearing subassemblies, and the Arduino MEGA galvanometer circuit schematic. Completion of the LPBF system fabrication is summarized below.

Chamber

The chamber was fully constructed by MIG welding the angle iron and steel plates together. Adaptable threaded gas ports were installed into the steel back plate. The entire structure was spray-painted black to effectively absorb radiation from the Nd:YAG laser as well as scattered energy reflected off the powder. Any identified discontinuities in the weld beads were sealed with Flex Seal. The rubber was mated to the exterior of the chamber frame in compliance with the design. Installation of the acrylic windows was completed on all sides of the chamber. 3-dimensional hanging supports for fixturing the galvanometer were attached to the steel beams that ran horizontally on the inside of the chamber. The door was completely fabricated and installed onto the chamber frame. The chamber leveling pegs were not fabricated.

Galvanometer

The galvanometer was fully assembled and placed within the 3D-printed housing. The sample code was programmed into the Arduino MEGA microcontroller and successfully executed its function, which was to turn the mirrors so that the laser was deflected in a square pattern on the build plate. The circuit was organized on the breadboard to be placed above the galvanometer housing. The hanging supports worked as intended to firmly fixture the galvanometer over the build plate.

Bed Leveling System

All electrical and mechanical components for the bed leveling system were purchased. The bed plate design was cut out into the aluminum bed plate. The steel base was milled to hold the support shafts and the stepper motor. The system was electrically tested, and the motor ran without problem. Although the bed leveling system is ready for completion, final fabrication was prohibited due to the pandemic situation. The bearing housings need to be JB welded onto the bed plate in order for the system fabrication to be complete.

5.2 LPBF System Testing

Various tests were proposed to be conducted on the prototype LPBF system before completion of the project. However, due to the inability to have access to the system components, these tests were not able to be completed.

The first test aims to expose weak spots in the structural frame of the LPBF prototype. This pressure test would involve connecting a hose line to one of the gas port nipples. With the windows and door sealed in place, a steady stream of water would fill up the chamber. Once the chamber was filled with water, any gaps in the weld beads or any unseen holes in the chamber would be exposed. These weak points can be Flex Sealed and the chamber should be retested to ensure all gaps are sealed. This will ensure the chamber is airtight as it is intended to be.

The next test that should happen once the bed leveling system is completed inside the chamber is to test the electrical set up of both the galvanometer and the bed leveling system. This test should ensure the code works properly between both systems and runs seamlessly through one Arduino Uno. This testing should ensure the galvanometer will home and position itself to project the beam onto the center of the bed plate. Next, the bed leveling system should lower to the snap switch, then reposition itself exactly 181 mm from the bottom of the galvanometer F-theta lens port. This is the working distance of the F-theta lens, so this distance is important to maintain the correct spot size of the laser beam. Next, the galvanometer should begin to run, drawing the design it is intended to draw. After each layer of design drawn by the laser, the z axis stepper motor should lower the bed plate by one step, to simulate a real 3D printing scenario. If the electrical components run correctly in the right sequence, then the electrical set up test is complete.

5.3 Conclusion and Future Work

Once the bed leveling system has been assembled, the LPBF chamber as designed for this project will be complete. Upon completion of these project, there are a few areas of improvement for the LPBF prototype. The code used to operate the galvanometer and the bed leveling system were for proof of concept. An updated code should be written for this system which has improved capabilities. These capabilities included allowing for a CAD model to be drawn by the galvanometer in a layer by layer fashion. This will allow for any design to be created with the laser galvanometer system. Additionally, the bed leveling system should be able to work seamlessly with the galvanometer and move in steps when a layer is completed. Another area of improvement for code would be on the bed leveling system. Since this is an experimental LPBF system, a varying step distance would be useful in terms of experimenting with different layer thicknesses.

The next step in improving the function and performance of the LBPF is to implement the retrofittable components that were recommended in this report. Once the proper equipment is retrofitted into place, this prototype will have capability of producing parts for experimentation in a safe manor. It is required that all proper retrofit options have been implemented into the LPBF chamber before the Nd:YAG laser is installed. As mentioned in this paper, this high-powered laser can cause a great deal of damage to life and property, so it is imperative that the other retrofit components are implemented before the Nd:YAG laser is active.

Lastly, the use of a commercial grade xy scanner galvanometer system would be beneficial for the prototype LPBF system. These galvanometers are made of high-grade material and precision machining and will function without fail for longer than the prototype galvanometer created for this project. No testing could be done to see the interaction between 3D printed ABS and a Nd:YAG laser, but after long term usage, the housing may begin to fail due to high temperature heat exposure. Additionally, the mirrors rotate on cheap, low voltage stepper motors, while real galvanometers use galvanometer motors. These types of motors are faster, and more precise in their movement capabilities. A commercial galvanometer for use with an Nd:YAG laser would improve the performance of the LBFP in the future.

References

2020 Types of 3D Printing Technology. (2020, March 19). Retrieved from https://all3dp.com/1/types-of-3d-printers-3d-printing-technology/

3DEXPERIENCE Platform. (2019). Powder Bed Fusion -- DMLS, SLS, SLM, MJF, EBM. Retrieved from https://make.3dexperience.3ds.com/processes/powder-bed-fusion.

Bergman, S. (2016, November 10). Beam diagnostics improve laser additive manufacturing. Retrieved from https://www.industrial-lasers.com/additive-manufacturing/article/16485613/beam-diagnostics-improve-laser-additive-manufacturing.

Cao, Y. & Zhu, D. (2017). Beam Steering. Retrieved from http://www.laserfocusworld.com/software-accessories/positioning-support-accessories/article/16556839/beam-steering-parallel-projection-galvo-scanning-enables-materials-processing-of-freeform-surfaces.

Chen, G. Design of Large Working Area F-Theta Lens. Retrieved October 11, 2019, from https://www.optics.arizona.edu/sites/optics.arizona.edu/files/msreport-gong-chen.pdf.

Gantry Systems: Working Outside the Envelope. (2018, September 11). Retrieved from https://www.macrondynamics.com/job-stories/gantry-systems-overview

Hecht, J. (2011). *Understanding Lasers*. John Wiley & Sons.

Knothe, M. T. (2018, April 17). The Value of Metal Additve Manufacturing with Diode Lasers. Retrieved from https://onlinelibrary.wiley.com/doi/pdf/10.1002/latj.201800011.

Laser Hazards-General. (2019). Retrieved 11 October 2019, from https://ehs.oregonstate.edu/laser/training/laser-hazards

Laser Standards and Classifications. (2019). Retrieved 11 October 2019, from https://www.rli.com/resources/articles/classification.aspx

Lee, H., Tham, N., & Singapore Center for 3D Printing. (2017). Lasers in Additive Manufacturing: A Review.

National Ignition Facility and Photon Science, Lawrence Livermore National Laboratory. How Lasers Work.

News, B. (2019). 7 Common System Types for Additive Manufacturing. Retrieved from https://www.kellertechnology.com/blog/7-common-system-types-for-additive-manufacturing/.

Powder Bed Fusion: Additive Manufacturing Research Group: Loughborough University. retrieved from https://www.lboro.ac.uk/research/amrg/about/the7categoriesofadditivemanufacturing/powderbedfusion/

Powder Bed Fusion (PBF) | Digital Alloys. (2019). Retrieved 11 October 2019, from https://www.digitalalloys.com/blog/powder-bed-fusion/

P.Bidare R.R.J.Maier R.J.Beck J.D.Shephard A.J.Moore, (2017), "An open-architecture metal powder bed fusion system for in-situ process measurements", Science Direct, https://www.sciencedirect.com/science/article/pii/S2214860416303700?via%3Dihub

SLM Solutions. General Terms and Conditions. Retrieved from http://www.slm-solutions.com/en/general-terms-and-conditions/.

Slotwinski, John, (2019). Retrieved 11 October 2019, from https://www.jhsph.edu/research/centers-and-institutes/johns-hopkins-education-and-research-center-for-occupational-safety-and-health/2017CHES/Slotwinski.Ginther_CHES0417.pdf

S. du Preez1, D.J. de Beer & J.L. du Plessis, (2019). Retrieved 11 October 2019, from http://www.scielo.org.za/pdf/sajie/v29n4/09.pdf

Spring, K. (2009). Introduction to Lasers. Retrieved from http://www.olympus-lifescience.com/en/microscope-resource/primer/lightandcolor/lasersintro/.